View metadata, citation and similar papers at core.ac.uk
brought to you by CORE
provided by Publications of the IAS Fellows

The hnRNP A1 homolog Hrp36 is essential for normal development, female fecundity, omega speckle formation and stress tolerance in *Drosophila melanogaster*

ANAND K SINGH and SUBHASH C LAKHOTIA*

Cytogenetics Laboratory, Department of Zoology, Banaras Hindu University, Varanasi 221 005, India

**Corresponding author (Fax, +91-542-2368-457; Email, lakhotia@bhu.ac.in)*

Hrp36/Hrb87F is one of the most abundant and well-characterized hnRNP A homolog in *Drosophila* and is shown to have roles in regulation of alternative splicing, heterochromatin formation, neurodegeneration, etc. Yet, *hrp36* null individuals were reported to be viable and without any apparent phenotype, presumably because of overlapping functions provided by Hrp38 and related proteins. Here we show that loss of both copies of *hrp36* gene slows down development with significant reduction in adult life span, decreased female fecundity and high sensitivity to starvation and thermal stresses. In the absence of Hrp36, the nucleoplasmic omega speckles are nearly completely disrupted. The levels of nuclear matrix protein Megator and the chromatin remodeller ISWI are significantly elevated in principal cells of larval Malpighian tubules, which also display additional endoreplication cycles and good polytene chromosomes. We suggest that besides the non-coding hsrω-n transcripts, the Hrp36 protein is also a core constituent of omega speckles. The heat-shock-induced association of other hnRNPs at the *hsrω* locus is affected in *hrp36* null cells, which may be one of the reasons for their high sensitivity to cell stress. Therefore, in spite of the functional redundancy provided by Hrp38, Hrp36 is essential for normal development and for survival under conditions of stress.

[Singh AK and Lakhotia SC 2012 The hnRNP A1 homolog Hrp36 is essential for normal development, female fecundity, omega speckle formation and stress tolerance in *Drosophila melanogaster*. *J. Biosci.* **37** 659–678] **DOI** 10.1007/s12038-012-9239-x

1. Introduction

The heterogeneous nuclear ribonucleoproteins (hnRNPs) are conserved in eukaryotes and are involved in a variety of RNA processing events, including splicing, transport and translation (Daneholt 2001; Guisbert *et al*. 2005; Martinez-Contreras *et al*. 2007; Olson *et al*. 2007; Blanchette *et al*. 2009; He and Smith 2009; Chaudhury *et al*. 2010; Han *et al*. 2010; Nilsen and Graveley 2010). In addition, some of them are known to be important in chromatin organization and regulation of gene expression (Piacentini *et al*. 2009) and to affect neurodegeneration (Sengupta and Lakhotia 2006; Sofola *et al*. 2007; Mallik and Lakhotia 2010). The different hnRNPs are grouped into 13 families in mammals, of which 11 are represented in *Drosophila* (Busch and Hertel 2012). The hnRNP A family in *Drosophila* is represented by Hrb87F/Hrp36, Hrb98DE/Hrp38 and Rb97D proteins (Busch and Hertel 2012). The Hrb27C/Hrp48 and Squid/Hrp40 of *Drosophila*, which share sequence and functional similarities with the Hrp36 and Hrp38 proteins, were considered as members of hnRNP A/B family by Blanchette *et al*. (2009), while Busch and Hertel (2012) grouped Squid/Hrp40 in the hnRNP D family. Hrp36 and Hrp38 seem to have overlapping functions so that a genetic null condition for any one of them is not lethal (Haynes *et al*. 1991; Zu *et al*. 1996). Hrp40 and Hrp48 share many common pre-mRNA targets with Hrp36 and Hrp38 during splicing (Blanchette *et al*. 2009).

It has been shown earlier that several hnRNPs including Hrp36, Hrp38, Hrp40, Bancal (hnRNP K/Hrb57A) and other related RNA-processing proteins including NonA (DBHS or *Drosophila* Behavior, Human Splicing protein family member; Kozlova *et al*. 2006), Sxl, etc., associate, in addition to their presence at many chromosome regions, with the nucleus

Keywords. 93D; hnRNP; ISWI; Megator; noncoding RNA; omega speckles; thermo-tolerance

Published online: 11 August 2012

limited non-coding hsrω-n transcripts of the *hsrω* gene in the nucleoplasmic omega speckles (Lakhotia *et al*. 1999; Prasanth *et al*. 2000; Jolly and Lakhotia 2006; Onorati *et al*. 2011). A disruption of omega speckles either in the absence of hsrω-n RNA in *hsrω* nulls or following down-regulation of these transcripts through RNAi results in a diffused distribution of the hnRNPs in nucleoplasm, and therefore, the hsrω-n RNA is considered to be essential for organization of omega speckles and association of the hnRNPs in the speckled nuclear compartment (Prasanth *et al*. 2000; Mallik and Lakhotia 2011; Lakhotia *et al*. 2012). Omega speckles are believed to function as storage sites for the unengaged hnRNPs and other related RNA-processing proteins and thus regulate their availability according to cellular needs (Lakhotia 2003; Jolly and Lakhotia 2006; Lakhotia 2011). Heat shock causes a dynamic redistribution of RNA Pol II and the omega-speckle-associated proteins inside the nucleus (Saumweber *et al*. 1980; Bonner and Kerby 1982; Zeng *et al*. 1997; Lakhotia *et al*. 1999; Prasanth *et al*. 2000; Boehm *et al*. 2003; Gerber *et al*. 2005; Lakhotia 2011). A recent study from our laboratory reported that altered levels of the hsrω transcripts affect the remobilization of hnRNPs, RNA Pol II and HP1 during recovery from heat shock, resulting in severely compromised thermo-tolerance (Lakhotia *et al*. 2012).

Earlier studies have shown that Hrp36, along with Hrp38, Hrp40 and Hrp48, affect alternative splicing of several transcripts in a sequence-specific manner (Zu *et al*. 1996; Borah *et al*. 2009; Blanchette *et al*. 2009; Nilsen and Graveley 2010). Piacentini *et al*. (2009) reported that Hrp36, PEP, HP1 and DDP1 dominantly suppress position effect variegation (PEV) and thus seem to be involved in heterochromatin formation. Hrp36 is also reported to be involved in neuronal development and its enhanced expression suppresses neurodegeneration in Fragile X-associated tremor/ataxia syndrome through its direct interaction with riboCGG repeats (Sofola *et al*. 2007). Depletion of *hrp36* leads to eye roughening with extra/fragmented photoreceptors and also enhances polyQ-induced neurodegeneration in *Drosophila* (Sengupta and Lakhotia 2006; Mallik and Lakhotia 2010). It is interesting that, in spite of the abundance of Hrp36 and its above noted roles in RNA processing, etc., its complete absence is reported to be without a phenotype and thus this protein has been suggested to be dispensable (Zu *et al*. 1996; Haynes *et al*. 1997). It is believed that the closely related Hrp38 provides functional redundancy so that a complete absence of Hrp36 is tolerated (Zu *et al*. 1996; Blanchette *et al*. 2009). Since the Hrp36 is a major constituent of omega speckles, we wanted to know the status of omega speckles in *hrp36* null individuals. Our present studies reveal that, like the hsrω-n transcripts, Hrp36 too is essential for formation of omega speckles since in its absence the hsrω-n RNA and the other hnRNPs do not assemble into speckled structures. Contrary to the earlier reports (Zu *et al*. 1996; Haynes *et al*. 1997), we found that a complete absence of this protein actually results in pleiotropic effects like developmental delay, reduced female fecundity, severely compromised stress tolerance, etc. Therefore, this protein is not completely dispensable.

2. Materials and methods

2.1 *Fly stocks and rearing condition*

Fly stocks were routinely reared on standard cornmeal-agar food medium at 24°C±1°C. In one set of experiments, larvae, pupae and adults were reared at 18°C or 24°C or 30°C (±1°C) on standard food. *Oregon* R^+ was used as the wild type. The *P{w*$^+$ *Tsr*$^+$*}/P{w*$^+$ *Tsr*$^+$*}; ry Df(3R)Hrb87F/ry Df(3R)Hrb87F* stock (Zu *et al*. 1996; Haynes *et al*. 1997), obtained from Dr S Haynes, was used as the *hrp36* null line. The entire *hrp36* coding region along with approximately 0.6 kb of *Tsr* gene (*CG9654, http://flybase.org),* encoding a Testis-specific RRM protein, is deleted in the *Df(3R)Hrb87F* chromosome, and therefore, *ry Df(3R)Hrb87F/ry Df(3R)Hrb87F* male flies are completely sterile, but *P{w*$^+$ *Tsr*$^+$*}/P{w*$^+$ *Tsr*$^+$*}; ry Df(3R)Hrb87F/ry Df(3R)Hrb87F* males and females carrying the *P{w*$^+$ *Tsr*$^+$*}* transgene on chromosome 2 are fertile (Haynes *et al*. 1997). The *P{w*$^+$ *Tsr*$^+$*}/P{w*$^+$ *Tsr*$^+$*}; ry Df(3R)Hrb87F/ry Df(3R)Hrb87F* flies will be referred to as *hrp36* null in the following.

2.2 *Developmental assay*

For developmental assay, eggs were collected at 2 h intervals from wild type or *hrp36* null flies and those hatching within a 2 h interval were collected and transferred to food vials. The vials were monitored at 24 h intervals until fly emergence for progression of development. To examine the effect of temperature, developmental assay was carried out at 18°C±1°C, 24°C±1°C and 30°C±1°C separately**.**

2.3 *Mouth hook preparation*

For mouth hook preparation, wild type and *hrp36* null larvae were taken out of the food vials at 24 h intervals after hatching of embryos. After washing with water, they were dried on blotting paper and fixed in glycerol : acetic acid (1:4) fixative at 60°C for 48 h, following which the mouth hooks and cuticle were separated and mounted in Hoyer's solution and kept at 60°C for 48 h. Mouth hooks of different age larvae were examined under light microscope. Mouth hooks of 25 larvae of each genotype were prepared at 24 h intervals till 96 h after hatching.

2.4 *Life span assay*

Flies of desired genotype were collected within 4 h of eclosion and transferred to fresh food vials at 24°C±1°C. Twenty-five flies were transferred in each vial. The number of dead flies was counted at 24 h intervals and the live flies were transferred to fresh food vials, without anesthetization, at 48 h intervals. Ten replicates of each set of experiment were examined.

2.5 *Fecundity assay*

To examine the role of Hrp36 in fecundity, following crosses of three days old 20 male and 20 female flies were set up: (a) wild type ♀ × wild type ♂, (b) *hrp36* null ♀ × wild type ♂, (c) wild type ♀ × *hrp36* null ♂ and (d) *hrp36* null ♀ × *hrp36* null ♂. Flies were allowed to lay eggs on cornmeal-agar food plates. Numbers of eggs laid during 24 h intervals in each plate were counted for the next seven days. Hatching of eggs was examined after 24 and 48 h from egg laying. Three replicates were kept for each set of experiment.

2.6 *Number of ovarioles in ovaries*

Ovaries from three- and ten-day-old wild type and *hrp36* null females, which were allowed to mate normally, were dissected out in Poels' salt solution (PSS; Lakhotia and Tapadia 1998), followed by staining in 2% aceto-carmine for 5 min, washing and mounting in 45% acetic acid with a lightly pressing coverslip. They were examined under a Nikon E800 microscope for the number of ovarioles in each of the two ovaries of a female.

2.7 *Starvation resistance assay*

Three-day-old wild type and *hrp36* null flies were transferred to empty bottles containing only water-soaked filter paper strips. The bottles were kept at 24°C±1°C and water-soaked filter paper strips were replaced at 8 h intervals. The number of dead flies was monitored at 8 h intervals after the starvation was started. Two replicates were carried out with each genotype.

2.8 *Thermo-tolerance assay*

Wild type and *hrp36* null actively wandering third instar larvae were heat-shocked at 37°C for 1 or 2 h. Larvae of the desired genotypes were collected in 1.5 mL microfuge tubes lined with moist filter paper and incubated in water bath maintained at 37°C±1°C for 1 or 2 h, following which the larvae were transferred to fresh food vials at 24°C±1°C and monitored until fly emergence. In another set, three-day-old healthy wild type and *hrp36* null flies were transferred in separate empty food vials and transferred to water bath maintained at 37°C±1°C for 1 h. The numbers of flies of each of the two genotypes that were immediately knocked down after heat shock and the numbers of flies that died during the next 5 days were counted. Each set of experiments was carried out at least in triplicate.

2.9 *Size and polyteny levels of wild type and hrp36 null larval Malpighian tubules (MT) and salivary glands (SG)*

To compare the width of MT and levels of polyteny in principal cells of MT, actively wandering wild type and *hrp36* null late third instar larvae were dissected in PSS and the MT were immediately fixed in freshly prepared 3.7% paraformaldehyde in PBS (137 mM NaCl, 2.7 mM KCl, 10 mM Na_2HPO_4, 1.8 mM KH_2PO_4, pH 7.4) for 20 min. After washing with PBS, tissues were stained with 4, 6-diamidino-2-phenylindole (DAPI, 1 μg/mL) and mounted on bridged slides in 1,4-diazabicyclo[2.2.2]octane (DABCO) antifade mountant. These were examined for measurement of width of MT under a Nikon E800 phase contrast microscope while nuclear diameter and total nuclear DAPI fluorescence intensity were measured from the confocal projection images.

To examine polytene chromosomes in principal cell nuclei, MT of actively wandering wild type and *hrp36* null late third instar larvae were dissected out in PSS, fixed in 3.7% formaldehyde in PBS followed by 3.7% formaldehyde in 45% acetic acid for 1 min each. They were washed briefly in 45% acetic acid and finally squashed under a coverslip in 45% acetic acid by tapping with rubber-ended pencil, followed by firm thumb pressure. Squash preparations of SG from actively wandering wild type and *hrp36* null late third instar larvae were also prepared similarly. Slides were briefly dipped in liquid nitrogen and the coverslips flipped off with a sharp blade. The slides were dipped immediately in 90% alcohol and after air-drying; the preparations were rehydrated in PBS, stained with DAPI and mounted in DABCO for examination under confocal microscope.

2.10 *Whole organ immunostaining*

MT from actively wandering wild type or *hrp36* null third instar larvae were dissected out in PSS and immediately fixed in freshly prepared 3.7% paraformaldehyde in PBS for 20 min and processed further for immunostaining with the desired antibodies (see below) as described earlier (Prasanth *et al*. 2000). Ovaries from wild type or *hrp36* null flies were stained with Tetramethyl Rhodamine Isothiocyanate (TRITC)-conjugated Phalloidin at 1:200 dilution to

localize the F-actin. Chromatin was counterstained with DAPI. Tissues were mounted in DABCO antifade mountant for confocal microscopy.

2.11 *Immunostaining of polytene chromosome squashes*

Actively wandering wild type and *hrp36* null late third instar larvae were heat shocked at 37°C for 40 min and their SG were dissected out in PSS either immediately or after 1 or 2 h recovery at 24°C. Parallel controls were maintained at 24°C. SG were dissected out from the control and treated larvae in PSS and transferred to 1% Triton X-100 in PBS for 30 s, following which they were treated consecutively with 3.7% formaldehyde in PBS and 3.7% formaldehyde in 45% acetic acid for 1 min each. Finally, the SG were incubated in 45% acetic acid for 1 min and squashed under coverslip in the same solution by first gentle tapping with rubber-ended pencil, followed by hard tapping and thumb pressure. Polytene chromosome spreads were examined under phase contrast microscope for appropriate spreading. Slides were briefly dipped in liquid nitrogen and the coverslips were flipped off with a sharp blade and the slides immediately dipped in 90% alcohol. These were processed further for immunostaining with the desired antibodies (see below) as described earlier (Lakhotia *et al*. 2012).

To examine the mode of association of proteins present at 93D locus after heat shock, one set of heat-shocked SG was treated with DNAse-free RNase A (1 mg/ml, Sigma-Aldrich, India) for 15 min at 24°C prior to fixation as described earlier (Lakhotia *et al*. 2012). The glands were processed further for polytene chromosome squash preparation and immunostaining as above.

2.12 *Western blotting*

Western blotting was done to estimate levels of HSP70, Hrb87F, NonA or β-tubulin. Following the desired treatment, protein samples were prepared either from whole larvae or a particular tissue (see Results) in SDS-PAGE sample buffer (Prasanth *et al*. 2000). After the electrophoretic separation on 10% SDS-PAGE, the polypeptides were blotted on PVDF membrane and processed for Western detection of the desired protein (see below) as described earlier (Mallik and Lakhotia 2009).

2.13 *Antibodies*

Primary antibodies used for immunostaining were mouse monoclonal anti-Hrp36 (P11; Saumweber *et al*. 1980) at 1:20 dilution, mouse monoclonal anti-NonA (Bj6, Saumweber *et al*. 1980) at 1:10 dilution, mouse monoclonal anti-Hrb57A (Q18; Saumweber *et al*. 1980) at 1:10 dilution, mouse monoclonal anti-Megator (BX34; Zimowska and Paddy 2002) at 1:10 dilution, mouse monoclonal anti-HP1 (C1A9; Developmental Studies Hybridoma Bank, USA) at 1:50 dilution, and rabbit anti-ISWI (Corona *et al*. 2007) at 1:2000 dilution. Appropriate secondary antibodies conjugated either with Cy3 (1:200, Sigma-Aldrich, India) or Alexa Fluor 488 (1:200; Molecular Probes, USA) or Alexa Fluor 546 (1:200; Molecular Probes, USA) were used to detect the given primary antibody.

The primary antibodies used for detection of HSP70, Hrb87F, NonA and β-tubulin in Western blots were 7Fb (Velazquez and Lindquist 1984; 1:1000 dilution), P11 (Saumweber *et al*. 1980; 1:200 dilution), Bj6 (Saumweber *et al*. 1980; 1:100 dilution) and E7 (Sigma-Aldrich, India; 1:200 dilution), respectively. The Western blots were developed with Horseradish peroxidase (HRP)-conjugated respective goat anti-rat HRP or goat anti-mouse HRP (Bangalore Genei, India) at 1:1000 dilution, using the Supersignal West Pico Chemiluminescent Substrate kit (Pierce, USA).

2.14 *RNA isolation and RT-PCR*

For semi-quantitative estimation of levels of the hsrω-n transcripts in wild type and *hrp36* null larval SG, RT-PCR was carried out with total RNA isolated from 20 pairs of SG, using the TRI Reagent as per the manufacturer's recommended protocol (Sigma-Aldrich, India). RNA pellets were resuspended in nuclease free water and incubated with 2U of RNase-free DNaseI (MBI Fermentas, USA) for 40 min at 37°C. First strand cDNA was synthesized using 2 µg of total RNA, 200U of Revert AidTM reverse transcriptase (MBI Fermentas, USA) and 80 pmol of oligo d(T)18 primer (New England Biolabs, USA). The samples were stored at −70°C until further use.

PCR was carried out for G3PDH transcripts, as loading control, using the forward 5′-CCACTGCCGAGGAGGT CAACTA-3′ and reverse 5′-GCTCAGGGTGATTGCG TATGCA-3′ primer pairs. The hsrω-n1 and hsrω-n2 (Mallik and Lakhotia 2011) cDNAs were co-amplified using forward primer P1 (5′-GGAAACAATGAAACCATACGC-3′) and reverse primer R1 (5′-TTGCGCTCACAGGAGATCAA-3′) pair. Another set of forward primer LP (5′-GGCAGA CATACGTACACGTGGCAGCAT-3′) in combination with the R1 reverse primer (see above) was used to amplify the total hsrω-n cDNA (Mallik and Lakhotia 2011). The thermal cycling parameters included an initial 4 min denaturation at 94°C followed by 30 cycles of 30 s at 94°C, 30 s at 60°C and 45 s at 72°C. Final extension was carried out at 72°C for 10 min. The PCR products were electrophoresed on 1.5% agarose gel with a 100 bp ladder marker (Bangalore Genei, India).

2.15 *RNA-RNA in situ hybridization*

MT from wild type and *hrp36* null late third instar larvae were dissected out in PSS, fixed in 4% paraformaldehyde for 2 min followed by incubation in 45% acetic acid for 4 min and partially squashed in same solution on poly-L-lysine-coated slide. After freezing in liquid nitrogen, the coverslip was flipped off and slide was dehydrated in 90% ethanol. FRISH was done with DIG-labelled antisense riboprobe from *pDRM30* clone that specifically detects hsrω-n transcripts following Prasanth *et al*. (2000). Chromatin was counterstained with DAPI and fluorescence was examined under confocal microscope.

2.16 *Confocal microscopy*

Zeiss LSM510 Meta laser scanning confocal microscope was used with Plan-Apo 40X (1.3-NA) or 63X (1.4-NA) oil immersion objectives. Quantitative estimates of the proteins on different regions of polytene chromosome or in intact nuclei were obtained with the help of profile and histo options of the Zeiss LSM Meta 510 software. All images were assembled using the Adobe Photoshop 7.0 software.

3. Results

In this study we compared several phenotypes of wild type and *hrp36* null (*P{w$^+$ Tsr$^+$}/P{w$^+$ Tsr$^+$}; ry Df(3R)Hrb87F/ry Df(3R)Hrb87F*) individuals. Since the *hrp36* null genotype also carries the *P{w$^+$ Tsr$^+$}* transgene, we examined possible effects of this transgene insertion on the phenotypes displayed by *hrp36* null individuals in pilot experiments. For this purpose, the phenotypes of *P{w$^+$ Tsr$^+$}/P{w$^+$ Tsr$^+$}; +/+* (only transgene insertion on chromosome 2), +/+; *ry Df(3R)Hrb87F/ry Df(3R)Hrb87F*, *P{w$^+$ Tsr$^+$}/P{w$^+$ Tsr$^+$}; ry Df(3R)Hrb87F/ry Df(3R)Hrb87F* and *P{w$^+$ Tsr$^+$}/P{w$^+$ Tsr$^+$}; ry Df(3R)Hrb87F/+* individuals were compared. The *+/+; ry Df(3R)Hrb87F/ry Df(3R)Hrb87F* (without the *Tsr* transgene insertion on chromosome 2 but *hrp36* null), (*P{w$^+$ Tsr$^+$}/P{w$^+$ Tsr$^+$}; ry Df(3R)Hrb87F/ry Df(3R)Hrb87F* (with the *Tsr* transgene insertion on chromosome 2 but *hrp36* null) displayed comparable phenotypic changes, except that the former males were also sterile as reported earlier (Haynes *et al*. 1997). Therefore, in all subsequent studies, the (*P{w$^+$ Tsr$^+$}/P{w$^+$ Tsr$^+$}; ry Df(3R)Hrb87F/ry Df(3R)Hrb87F*) genotype was used as *hrp36* null.

3.1 *Absence of Hrp36 protein delays development and affects viability*

We examined the time taken by *hrp36* null and wild type from hatching of embryos to pupation when grown at 18°C, 24°C or at 30°C (±1°C). Eggs of the two genotypes that hatched within a period of 2 h were selected for monitoring their subsequent development at 24 h intervals. As the data in figure 1 show, there is some variation in the time required by different larvae of a given genotype to pupate. However, the *hrp36* null larvae always started pupating much later than the wild type larvae. Interestingly, the time gap between first and last pupation was significantly greater in *hrp36* null than in wild type and increased with lower rearing temperature (figure 1). A comparable delay in the emergence of adults was also noted for the *hrp36* null pupae (not shown).

To examine if certain larval stages were specifically affected, we examined the number of teeth on mouth hooks of 24°C reared larvae at 24 h intervals after hatching. After 48 h of hatching, 100% of the wild type larvae (N=25) reached second instar stage while only 20% of the *hrp36* null larvae (N=25) were at the second instar stage. After 72 h of hatching, 100% wild type larvae reached third instar stage compared to only 15% *hrp36* null larvae. Only after 96 h, all the *hrp36* null larvae were at the third instar stage. Thus, each instar's duration is extended in *hrp36* nulls.

Another interesting difference between the wild type and *hrp36* null larvae was the site of pupation. 57% of the *hrp36* null larvae (N=212) pupated on the surface of food, while in the wild type only 3% larvae (N=289) pupated on food and the rest pupated on drier surfaces away from the food.

As reported earlier by Haynes *et al*. (1997), no significant larval (figure 1) or pupal (not shown) lethality was observed in *hrp36* nulls that were reared at 24°C or at 18°C. However, the *hrp36* nulls grown at 24°C appeared a little weak and lethargic compared to the wild type, and with age, their weakness increased substantially. Life span assay revealed that the median life span of *hrp36* null flies at 24°C was significantly less (23.9±1.6, N=250) than in the wild type (30.7±1.6, N=250) flies reared in parallel.

The *hrp36* null pupae and adults were very sensitive to rearing at 30°C. Nearly 70% of 30°C reared *hrp36* null larvae died as late pupae or pharates or soon after emergence (figure 2A and B). The surviving flies were very weak, unable to fly, laid very few eggs and died within a few days. Wild type larvae reared at 30°C did not show any significant pupal or adult death.

3.2 *hrp36 null females have reduced fecundity and show abnormal ovarian follicles*

Since the number of progeny in the *hrp36* null stock appeared much less than in wild type stock grown in parallel and since the above data indicated little larval or pupal death of *hrp36* null progeny, we examined to check if the fecundity of *hrp36* null females was compromised. Examination of ovaries in wild type and *hrp36* null females revealed that unlike in wild type females, one of the two ovaries in *hrp36*

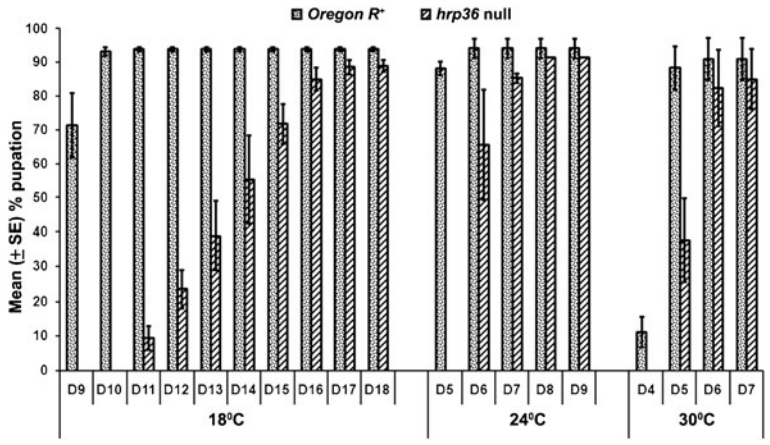

Figure 1. Absence of Hrp36 protein substantially delays development. Graphical presentation of the time (in days, X-axis) of pupation after hatching of wild type and *hrp36* null first instar larvae reared at 18°C (N=289 and 212, respectively), 24°C (N=826 and 651, respectively) or at 30°C (N=578 and 165, respectively). The Y-axis shows mean percentages (±S.E., based on three replicates) of larvae that pupated till a given day.

null females was often much smaller than the other (figure 3A–C). The numbers of ovarioles (sum of the two ovaries) was also significantly less in *hrp36* null females compared to that in same age (3 or 10 days old) wild type females (table 1).

We counted the numbers of eggs laid by wild type or *hrp36* null females mated with wild type males. It was seen that between day 3 to day 9 of adult life, the *hrp36* null females always laid fewer eggs than corresponding age wild type females (figure 3D). In another set, we compared the hatchability of eggs laid by wild type females that were mated with either wild type or *hrp36* null males and by *hrp36* null females that were mated with wild type or *hrp36* null males. It was seen that eggs laid by *hrp36* null mothers suffered a greater (about 17–18%) embryonic death irrespective of their fathers being wild type or *hrp36* null males (figure 3E). It is interesting that the *Df(3R)Hrb87F/+* zygotes suffered embryonic death only when the mother's genotype was *Df(3R)Hrb87F/Df(3R)Hrb87F* since the *Df (3R)Hrb87F/+* eggs laid by wild type females that were mated with *Df(3R)Hrb87F/Df(3R)Hrb87F* males did not show significant embryonic lethality (figure 3E). This clearly indicates a maternal effect of *hrp36* null genotype.

Further examination of ovarioles revealed additional defects. Organization of F-actin in the thin circular muscles of the epithelial sheath surrounding each of the ovarioles in

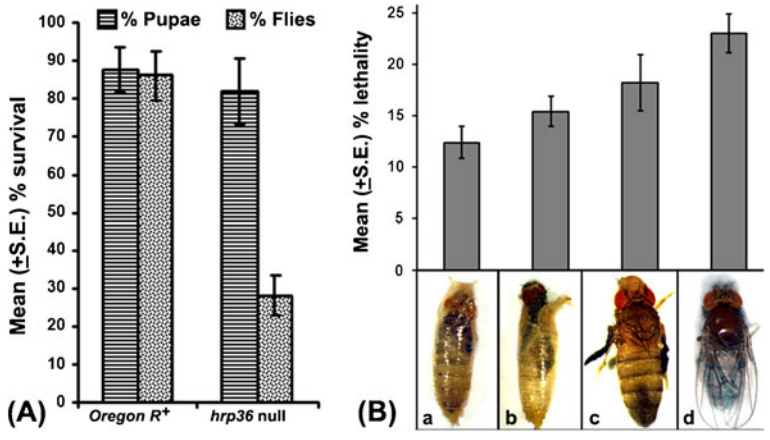

Figure 2. The *hrp36* nulls are sensitive to rearing at 30°C. (**A**) Graphical presentation showing mean (±S.E., 3 replicates) percentages of wild type (N=578) and *hrp36* null (N=165) larvae (X-axis) that pupated and subsequently emerged as adult flies (Y-axis) when reared at 30°C±1°C. (**B**) Shows mean (±S.E., 20 replicates of 25 pupae each) percentages of *hrp36* null pupae which died as late pupae (**a**), pharates (**b**), freshly emerged flies (**c**) or within 3 days after emergence (**d**) when reared from egg hatching onwards at 30°C±1°C.

Table 1. Ovaries of *hrp36* null females have fewer ovarioles than in wild type flies of comparable age

Mean (±S.E.) no. of ovarioles per female		
Age of female	Wild type	*hrp36* null
3 days	17.44±0.25	11.95±0.41*
10 days	16.05±0.23	10.79±0.44*

* The mean number of ovarioles in *hrp36* null ovaries is significantly ($P<0.001$) less than that in corresponding age wild type females; N=30 females for each genotype and age.

hrp36 null ovaries was altered. Unlike the thin and rather discontinuous actin filaments in the epithelial sheath covering the wild type ovarioles (figure 3F), continuous and a higher number actin filaments wrapped the entire ovariole in *hrp36* null ovaries (figure 3G). The F-actin layer at the interface of follicle and nurse cells in *hrp36* null chambers was thinner than in the wild type egg chambers (see insets in figure 3 F and G). Further, many of the *hrp36* null ovarioles did not contain egg chambers beyond stage 7–8 (figure 3G), possibly due to a high incidence of apoptosis in *hrp36* null flies (figure 3G and I). Ring canals appeared normal in the mutant egg chambers.

Organization of chromatin in the *hrp36* null ovarioles was also affected. As reported by King (1970) the highly endoreplicated chromosomes of nurse cell nuclei in stage 6 and later chambers appear as fully dispersed chromatin (inset in figure 3H). However, in *hrp36* null egg chambers, the highly endoreplicated chromatin remained more condensed in blob-like structures even in later stages (inset in figure 3I), similar to that reported earlier for *Squid*, *hrb27C* or *otu* mutants (King *et al*. 1981; King and Storto 1988; Goodrich *et al*. 2004).

3.3 *Malpighian tubules are enlarged in width with higher levels of polyteny while salivary gland chromosomes show distinct telomere elongation in hrp36 null larvae*

The MT of *hrp36* null larvae were nearly two times thicker (figure 4C, D, E) than in the wild type (figure 4A, B, E). Correspondingly, the nuclei in the polytenized principal cells of MT of *hrp36* null larvae were also nearly two times larger than in *Oregon* R^+ larvae of comparable stage (figure 4F–H). Squash preparations of late third instar *hrp36* null larval MT revealed well-spread polytene chromosomes with distinct band/interband organization (figure 4J) compared to the poorly polytenized chromosomes seen in wild type MT (figure 4I). Total DAPI fluorescence of the principal cell nuclei in *hrp36* null larval MT was also greater than in the corresponding wild type MT (figure 4K). The size of the chromocentre, which is known to be not involved in endoreplication (Lakhotia 1974, 1984), was comparable in wild type and *hrp36* null larvae. The sizes of polytene chromosomes in SG were comparable between wild type and *hrp36* null (figure 4L-N). Their total DAPI fluorescence values were also comparable (data not presented). Interestingly, however, all the polytene chromosome arms in all *hrp36* null larval SG nuclei showed distinct elongation of telomeres when compared with wild type chromosome arms tips and the extended telomeres in *hrp36* nuclei displayed occasional association of different telomeric regions (figure 4L–N).

3.4 *Hrp36 is essential for organization of the omega speckles*

The Hrp36 is one of the major hnRNPs which is physically associated with the non-coding hsrω-n transcripts in the nucleoplasmic omega speckles (Prasanth *et al*. 2000; Lakhotia *et al*. 2012). In order to find out the role of Hrp36 in organization of omega speckles, we examined nuclear distribution of hsrω-n transcripts and the omega speckle interacting proteins like NonA (Onorati *et al*. 2011) and Bancal/Hrb57A (Prasanth *et al*. 2000) in the principal cells of MT in wild type and *hrp36* null late third instar larvae.

In situ hybridization of hsrω-n specific riboprobe to MT cells revealed that unlike the specific localization of the hsrω-n transcripts in the nucleoplasmic omega speckles and the site of transcription in wild type MT nuclei (figure 5A and B), the *hrp36* null MT cells displayed few omega speckles. Instead, the hsrω-n transcripts in these cells were distributed more or less in a diffuse manner in the nucleoplasm with a prominent cluster at the site of transcription (figure 5C and D).

Immunostaining of NonA and Bancal proteins also revealed almost complete disruption of the omega speckles in MT nuclei of *hrp36* null larvae. Both these proteins were, like the hsrω-n transcripts, diffused through the nucleoplasm (figure 5G, H, K and L) rather than as individual small nucleoplasmic speckles seen in wild type (figure 5E, F, I and J). In addition, these proteins were also present in small clusters on chromatin regions. Similar to MT principal cell nuclei, speckled pattern of these hnRNPs was also disrupted in MT stellate and other polytene and diploid cell nuclei in gut (not shown).

3.5 *Absence of Hrp36 affects localization of nuclear matrix protein Megator and chromatin remodelling protein ISWI in MT nuclei*

Earlier studies have reported a role of hnRNP A in organization of the nuclear matrix (He *et al*. 1991; Zimowska *et al*. 1997) in higher eukaryotes. Therefore, we compared the localization of a nuclear matrix protein Megator in MT

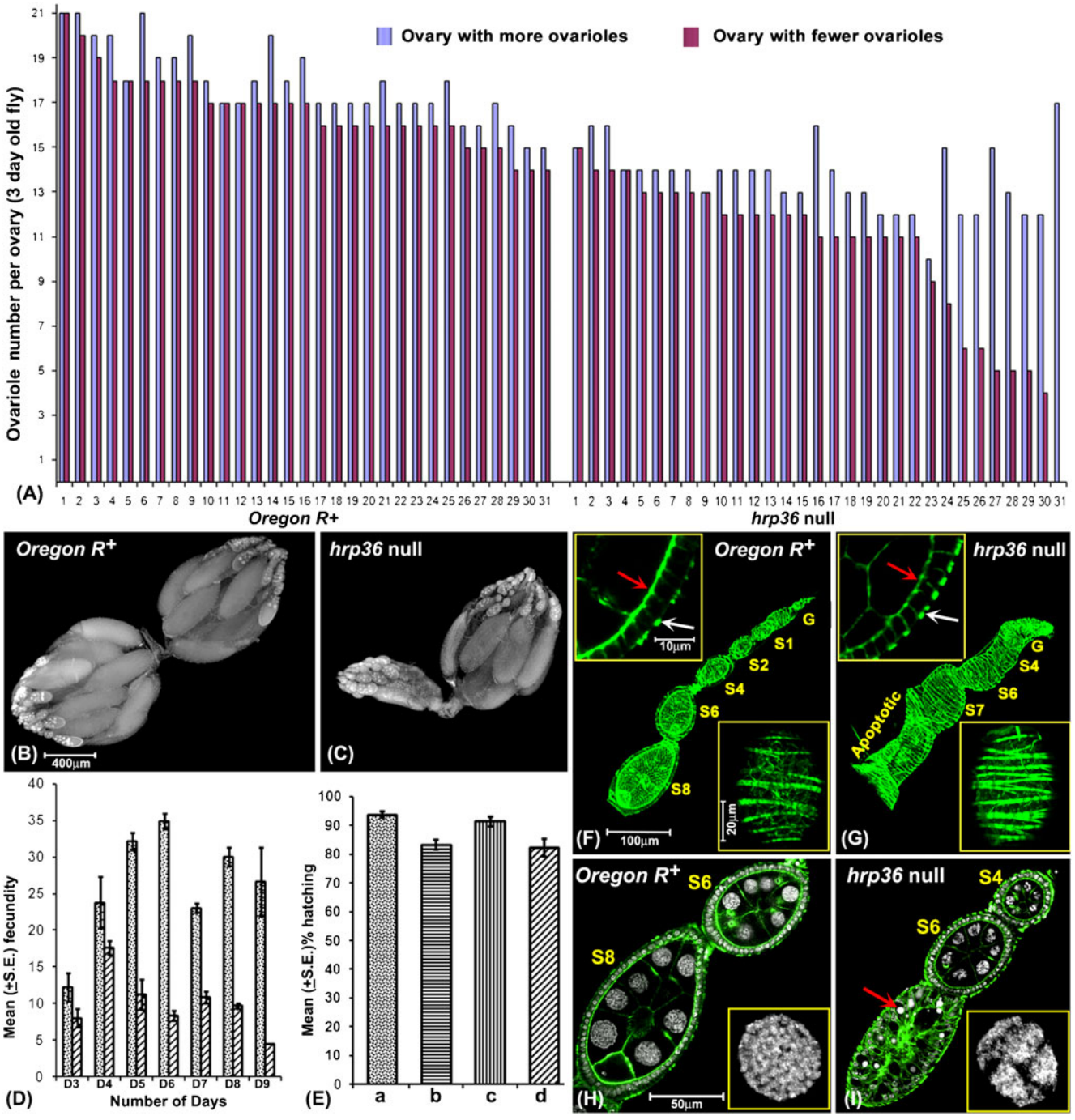

principal cell nuclei of *hrp36* null and wild type. Interestingly, while in wild type nuclei, the Megator was seen in small clusters of speckles in the nucleoplasm (figure 6A), in the *hrp36* null cells (figure 6B), this protein was present in larger clusters in the interchromatin space with less distinct punctate distribution (figure 6B). However, the presence of Megator as a rim at the nuclear periphery was similar in the *hrp36* null and wild type nuclei (figure 6A and B).

The nucleoplasmic distribution of ISWI protein, a component of chromatin remodelling complexes, was also affected in *hrp36* null cells since its punctated distribution in nucleoplasm in wild type nuclei (figure 6D) was not seen in *hrp36* null nuclei (figure 6E).

The immunofluorescence for Megator as well as ISWI proteins in the *hrp36* null MT nuclei appeared to be much greater than in the wild type nuclei (figure 6A, B, D and E).

Figure 3. Absence of Hrp36 affects fecundity and oogenesis. (**A**) Graphical presentation of the numbers of ovarioles in each of the two ovaries in 3-day-old *Oregon* R^+ (left, N=31) and *hrp36* null (right, N=31) females; the pairs of bars (blue and magenta) represent the numbers of ovarioles in each of the two ovaries of an individual fly; these are arranged in decreasing order keeping the ovary with lesser number of ovarioles (magenta bars) as reference. DAPI stained (white) ovaries of 7-day-old wild type (**B**) and *hrp36* null (**C**) female flies. Note the fewer ovarioles (also see Table 1) and mature eggs and consequently much smaller size of one of the two ovaries in *hrp36* null females. (**D**) Graphical presentation showing the mean numbers of eggs laid/female (fecundity) on different days (X axis) by wild type ♀ × wild type ♂ (stippled bars) and by *hrp36* null ♀ × wild type ♂ (hatched bars). (**E**) Graphical presentation showing the mean percentage hatching of eggs laid by (a) WT ♂ × WT ♀ (93.9%), (b) WT ♂ × *hrp36* null ♀ (83.4%), (c) *hrp36* null ♂ × WT ♀ (91.5%) and (d) *hrp36* null ♂ × *hrp36* null ♀ (82.3%) parents. (**F** and **G**) Phalloidin stained (green) single ovarioles of wild type (**F**) and *hrp36* null (**G**) flies showing higher numbers of circular muscle fibres in the epithelial sheath in the *hrp36* null chambers at different stages (G= germarium, S1-S8, stage 1 to stage 8, respectively); on the basis of DAPI staining (not shown), the chamber behind the S7 in (**G**) appears apoptotic; insets at the lower right corners in (**F**) and (**G**) are higher magnifications projection images of top three optical sections of Phalloidin stained stage 6 chambers, while the insets on upper left corners show higher magnification image of single optical sections of the follicle cell layer and parts of the underlying nurse cells of Phalloidin stained stage 6 egg chambers of respective genotype; the red arrows point to the F-actin layer at the nurse cell face of follicle cell layer, while the white arrows point to the sectional view of circular muscle fibres in the external epithelial sheath. (**H** and **I**) Single confocal sections of ovarioles showing distribution of F-actin (green) and chromatin (DAPI stained, white) in different stages of egg chambers from wild type (**H**) and *hrp36* null (**I**) ovaries: red arrow in (**I**) points to an apoptotic chamber in *hrp36* null ovariole. The images in insets in (**H**) and (**I**) are high-magnification projection images of DAPI stained stage 7 nurse cell nuclei showing properly dispersed chromosomes in wild type but blob-like arrangement of chromatin in *hrp36* null nurse cells.

In order to know if the enhanced immunostaining for these proteins in *hrp36* null principal cell nuclei was correlated with their increased DNA content, we compared the ratios of the nuclear Megator (excluding the nuclear rim associated fluorescence) or ISWI and nuclear DNA (DAPI fluorescence) in wild type and *hrp36* null MT nuclei (figure 6C and F). This comparison clearly revealed that compared to the wild type, the increase in levels of Megator and ISWI in principal cells of MT of *hrp36* null larvae is much more than the increase in DNA.

3.6 *Absence of Hrp36 affects starvation and thermal stress tolerance*

3.6.1 *Starvation stress:* Three-day-old *Oregon* R^+ and *hrp36* null flies were starved and their survival monitored at 8 h intervals. As seen from survival curves in figure 7A, death of starved *hrp36* null flies started as early as 24 h of starvation, while the *Oregon* R^+ flies began to die only after 48 h of starvation. After 50 h of starvation, ~90% *hrp36* null flies were dead while in the case of *Oregon* R^+ flies, a comparable percentage of death was observed after ~90 h of starvation (figure 7A).

3.6.2 *Thermo-tolerance:* To examine a role of Hrp36 in thermo-tolerance, actively wandering third instar wild type and *hrp36* null larvae were heat-shocked at 37°C for 1 or 2 h and their survival was monitored until the emergence of flies. Data from three replicates revealed that *hrp36* nulls are more thermo-sensitive since following 1 h exposure to 37°C, only 65% of the larvae survived to adulthood compared to emergence of 97% of similarly treated wild type larvae. Likewise, only 25% of *hrp36* null larvae exposed to 37°C for 2 h emerged as flies in contrast to emergence of 88% wild type larvae (figure 7B). In the absence of Hrp36 protein, adult flies also showed greater thermo-sensitivity since after 1 h of heat shock at 37°C all the *hrp36* null flies were knocked down compared to the knock down of only 26% of the wild type flies (figure 7C). Five days after the heat shock, compared to 95% survival of wild type flies, only 53% *hrp36* null flies survived (figure 7C).

3.7 *Absence of Hrp36 protein does not affect the heat shock induced synthesis of Hsp70*

In order to see if the heat shock response was compromised because of the complete absence of Hrp36 protein, we examined the inducibility of Hsp70 in response to heat shock. As shown in figure 8, the status of Hsp70 in control, heat shocked and 2 h recovered wild type and *hrp36* null larvae was comparable. As noted below, the different heat shock puffs were also comparably induced in wild type and *hrp36* null larval SG (figure 9).

3.8 *Absence of Hrp36 protein affects the heat-shock-induced redistribution of omega-speckle-interacting proteins*

Heat shock results in disappearance of the nucleoplasmic omega speckles and at the same time, most of the hnRNPs and other proteins associated with omega speckles and chromosome regions get relocalized to the *93D* or *hsrω* site (Prasanth *et al*. 2000). To investigate the role of Hrp36 in this mobilization, we examined localization of NonA, which is one of the omega-speckle-interacting proteins (Onorati *et al*. 2011), on salivary gland polytene chromosome spreads from actively wandering third instar wild type and *hrp36* null larvae. Under unstressed condition, the amount of NonA protein at the 93D locus in *hrp36* null polytene chromosomes

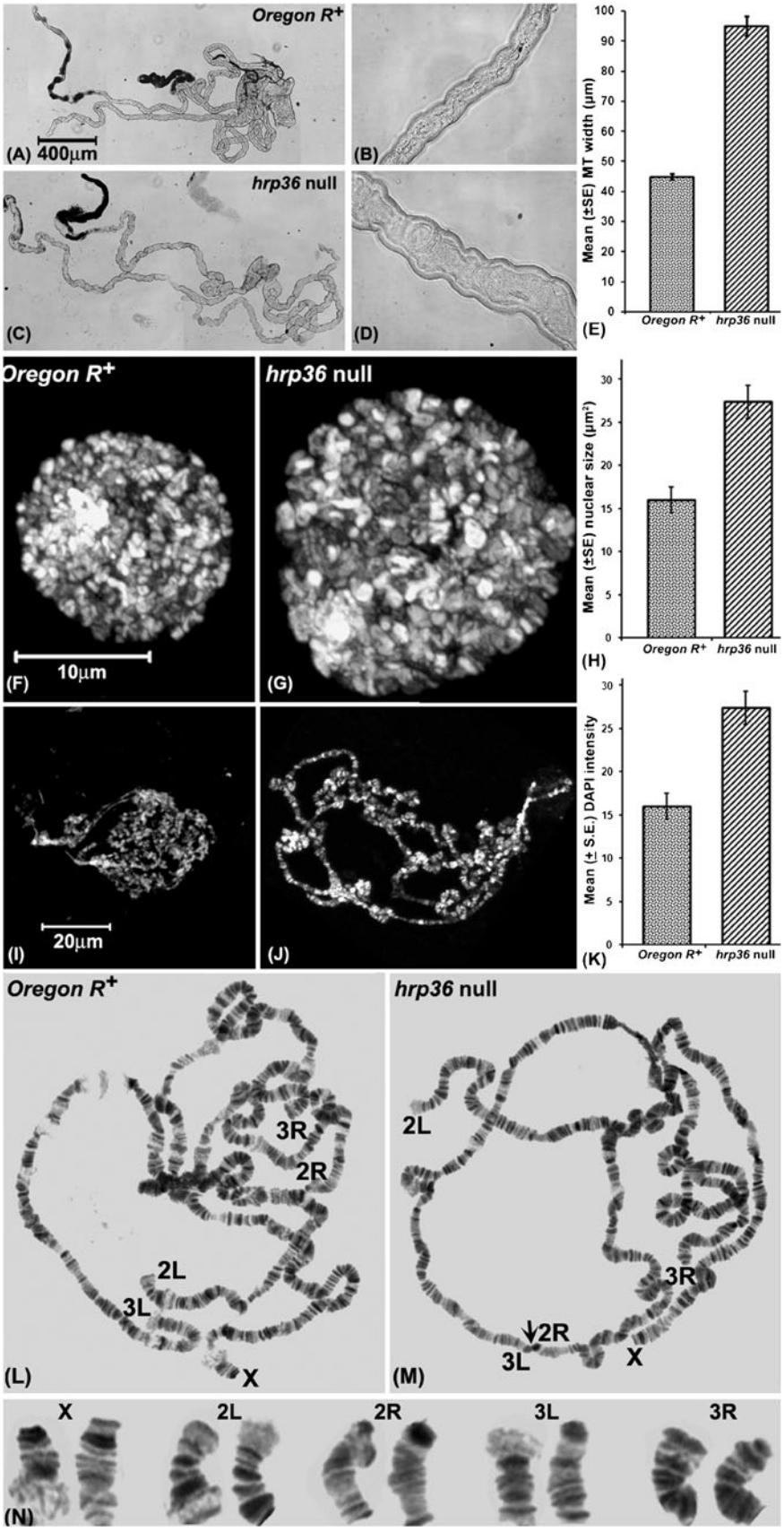
Oregon R+
(A) 400μm
(B)
hrp36 null
(C)
(D)
Mean (±SE) MT width (μm)
Oregon R+
hrp36 null
(E)
Oregon R+
hrp36 null
10μm
(F)
(G)
Mean (±SE) nuclear size (μm²)
(H)
20μm
(I)
(J)
Mean (± S.E.) DAPI intensity
(K)
Oregon R+
3R
2R
2L
3L
X
(L)
hrp36 null
2L
3R
2R
3L
X
(M)
X
2L
2R
3L
3R
(N)

◀ **Figure 4.** Malpighian tubules (MTs) are enlarged because of increased polyteny of the principal cells in *hrp36* null larvae. Phase contrast images of MT from wild type (**A** and **B**) and *hrp36* null (**C** and **D**) at lower (**A** and **C**) and higher (**B** and **D**) magnifications. Graphical presentation of mean (±S.E, N=25 for each value) width of MTs from *Oregon* R^+ and *hrp36* null (E) larvae. Confocal projection images of DAPI-stained MT principal cell nuclei in intact MTs from *Oregon* R^+ (**F**) and *hrp36* null (**G**) late third instar larvae. Graphical presentation of mean (±S.E, N=50 for each value) nuclear diameter of polytene nuclei from *Oregon* R^+ and *hrp36* null larval MT (**H**). Confocal images of DAPI-stained squash preparations of polytene chromosomes in MT principal cells from *Oregon* R^+ (**I**) and *hrp36* null (**J**) late third instar larvae. Graphical presentation of the mean (±S.E, N=8 for each value) total nuclear DAPI fluorescence of polytene nuclei from wild type and *hrp36* null larval MT (**K**). Salivary gland polytene chromosomes of wild type (**L**) and *hrp36* null (**M**) larvae showing telomere association (arrow) and telomere elongation in *hrp36* null; tips of different chromosome arms (X, 2L, 2R, 3L and 3R) are marked. Magnified images of pairs of telomeric regions of the different long arms (X, 2L, 2R, 3L and 3R) from wild type (left) and *hrp36* null (right) chromosome spreads in (**L**) and (**M**), respectively, are presented in (**N**) to show the substantially elongated telomeres in *hrp36* null chromosomes.

was distinctly less than that in wild type (figure 9A and B). Following heat shock, the NonA protein moved away from most of the chromosomal sites in wild type cells and strongly accumulated at the 93D puff; after 2 h recovery from heat shock the distribution of NonA resembled the pre-stress condition (figure 9C and E). It is notable that the level of NonA protein at the 93D site in heat-shocked *hrp36* null cells was always much less than in wild type cells, while that on the other chromosomal regions was greater than in heat shocked wild-type chromosomes (figure 9D and F). We quantitated the amount of NonA protein at different cytological regions including the 93D, 87C and 87A puffs and a segment of right arm of chromosome 3 (100F to 93E region) in polytene chromosome spreads of wild type and *hrp36* null SG following heat shock and after 2 h recovery from heat shock. As shown in figure 9G, while the level of NonA at

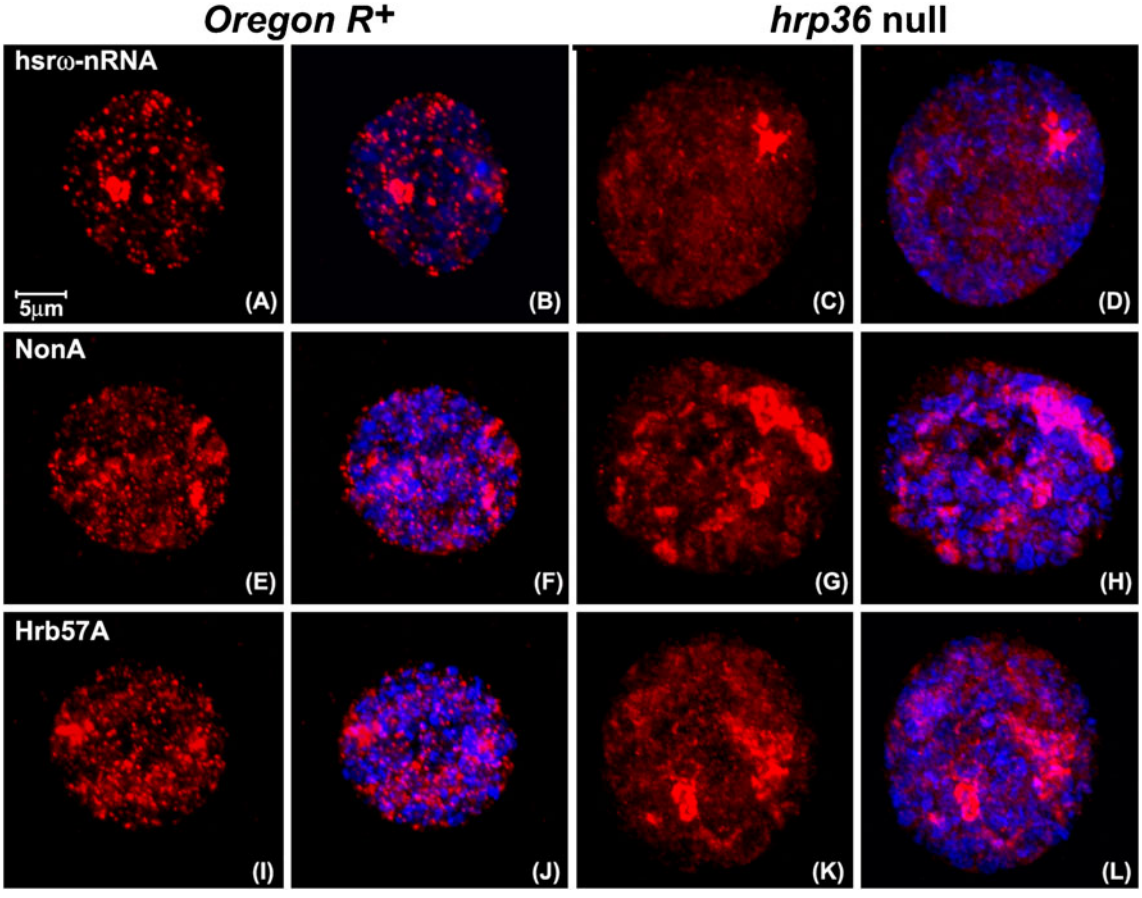

Figure 5. Typical omega speckles do not form in the absence of Hrp36. Confocal projection images to show *in situ* localization of hsrω-n RNA (red, **A**–**D**), NonA (red, **E**–**H**) and Hrb57A or Bancal (red **I**–**L**) in Malpighian tubule principal cell nuclei of different genotypes (noted above columns). Chromatin, counterstained with DAPI (blue), is seen in the merged images in **B**, **D**, **F**, **H**, **J** and **L**.

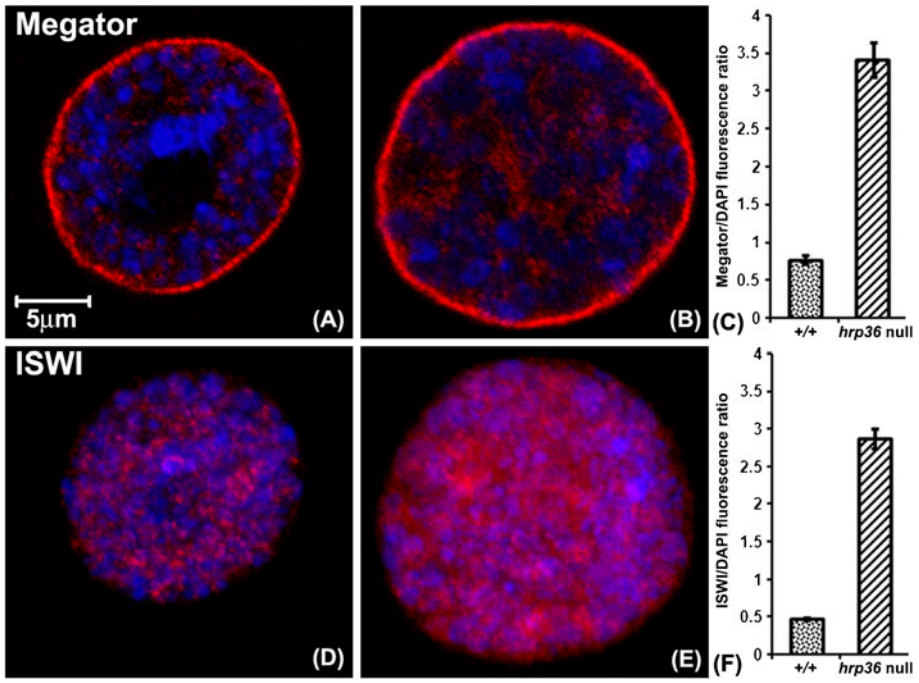

Figure 6. Absence of Hrp36 affects the localization and abundance of nuclear matrix and chromatin remodelling proteins. Confocal projection images showing immunolocalization of Megator (red, **A** and **B**) and ISWI (red, **D** and **E**) in unstressed MT principal cell nuclei of wild type (**A** and **D**) and *hrp36* null (**B** and **E**) larvae. DNA is stained with DAPI (blue). (**C**) Graphical representation of the relative levels of Megator (excluding the peripheral nuclear rim) in MT nuclei of wild type and *hrp36* null larvae, expressed as ratios of Megator and DAPI fluorescence in a nucleus (N=60 optical medial sections from 20 nuclei for each genotype). (**F**) Graphical representation of the relative levels of ISWI in MT nuclei of wild type and *hrp36* null larvae, expressed as ratios of ISWI and DAPI fluorescence in a nucleus (N=20 for each genotype).

93D puff in heat-shocked *hrp36* null cells was approximately 50% of that in wild type cells, it was much more abundant at the 87A and 87C puffs and the 100F to 93E chromosome region in *hrp36* null than in the wild type. Interestingly, after a 2 h recovery from heat shock, the levels of NonA on the 3R segment were comparable in *hrp36* null and wild type cells but the 93D site showed much less fluorescence. Compromised clustering of RNA-processing proteins during heat shock was also observed in other polytene as well as diploid cell nuclei of *hrp36* null (not shown).

In order to see if the varying levels of NonA at the 93D puff site and other chromosome regions was related to any difference in the total cellular levels of this protein, we estimated NonA and Hrp36 in wild type and *hrp36* null control and heat-shocked larvae and in those that had recovered for 2 h from the heat shock through Western blotting. The levels of NonA remained constant and equal in all conditions in wild type and *hrp36* null larvae (figure 9H). The levels of Hrp36 in wild type larvae also did not change under the different experimental condition and, as expected, the *hrp36* null larval samples did not show any trace of signal in any of the lanes.

We also examined the localization of two chromatin remodelling proteins, viz heterochromatin protein HP1 and ISWI, on heat-shock-induced 87A, 87C and 93D puffs in wild type and *hrp36* null polytene chromosome spreads. As reported earlier (Lakhotia *et al*. 2012), HP1 protein is present at the 93D site in control cells (not shown). Heat shock causes a strong accumulation of HP1 at the 93D puff in wild type (figure 10A). Significantly, while the level of HP1 in control *hrp36* null polytene cells was comparable to that in wild type control cells, in the heat-shocked *hrp36* null cells, much less HP1 protein was present at the 93D puff than in wild type (figure 10B). As also reported earlier (Lakhotia *et al*. 2012), HP1 was found to be present in very small amounts at the 87A and 87C puffs in wild type as well as the *hrp36* null cells (figure 10A and B).

In agreement with a previous report (Sala *et al*. 2008), ISWI was detectably present at the 87A and 87C sites in unstressed wild type and control cells (not shown) but was completely absent in both genotypes at the heat-shock-induced 87A and 87C puffs (figure 10C and D). ISWI protein was distinctly seen at the 93D site in control cells of both genotypes (not shown), but unlike its disappearance at the 87A and 87C puffs, its levels at the 93D puff increased significantly after heat shock in wild type as well as *hrp36* null polytene cells. Interestingly, unlike the hnRNPs and HP1,

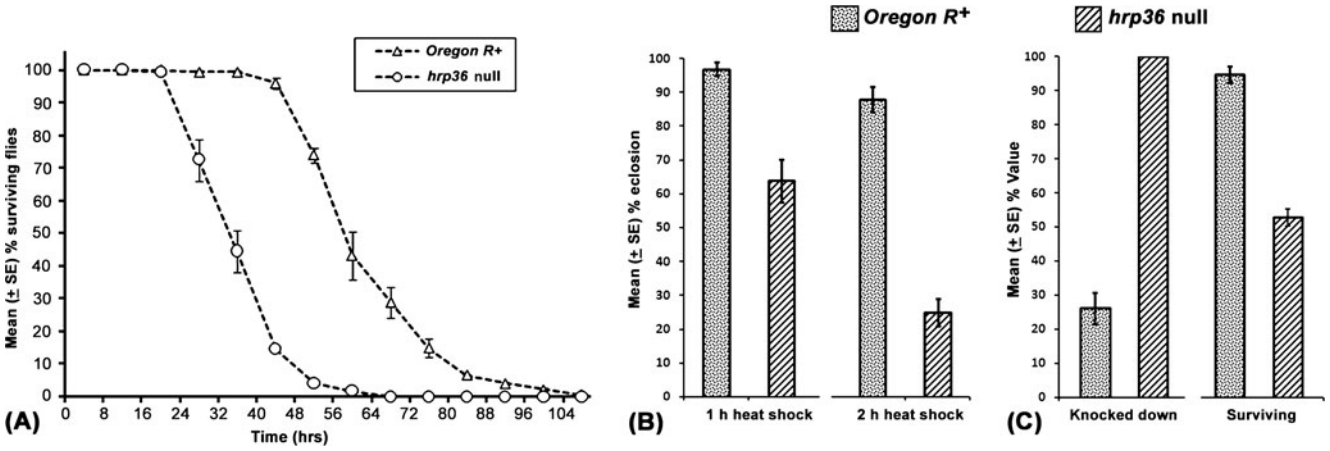

Figure 7. The *hrp36* null flies are highly sensitive to starvation and heat stresses. (**A**) Survival curves of *Oregon R*$^{+}$ (N=172) and *hrp36* null (N=297) flies measured at 8 h intervals after beginning of the starvation treatment. The mean (±S.E.) % surviving flies (Y-axis) for each time point (X-axis) is based on two replicates. (**B**) Graphical presentation of mean (±S.E., based on 3 replicates) % of *Oregon R*$^{+}$ (N=200) and *hrp36* null (N=200) larvae that emerged as young flies after heat shock for 1 or 2 h (X-axis) at late third instar stage. (**C**) Graphical presentation showing mean (±S.E., based on 2 replicates) percentage of 3-day-old *Oregon R*$^{+}$ (N=220) and *hrp36* null (N=322) flies that were knocked down just after heat shock (left) and of those surviving for the next 5 days (right). The mean percentage values (Y-axis) are based on two replicates.

the strong accumulation of ISWI at the 93D puff following heat shock was comparable in wild type and *hrp36* null larvae. ISWI protein was present at low levels at the other heat shock gene sites in control cells of both genotypes with no appreciable change detectable in any of the genotypes following the heat shock.

In view of the comparable levels of ISWI at the 93D puff site in *hrp36* null and wild type polytene chromosomes but much less accumulation of NonA and HP1 after heat shock in the former, we examined if the association of these proteins at 93D locus is sensitive to RNase. Interestingly, RNase treatment of live heat-shocked glands removed most of the NonA and HP1 proteins from the 93D puff site while immunostaining for ISWI at the 93D puff site was not affected by the RNAse treatment (figure 10E–G). This shows that while NonA and HP1 accumulate through their association with RNA at the 93D site after heat shock, ISWI directly binds with DNA at 93D locus.

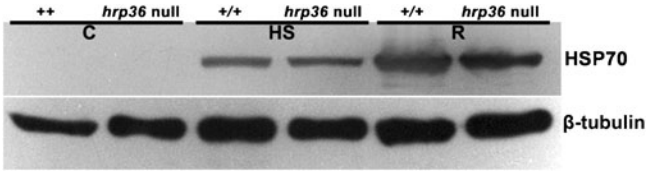

Figure 8. Levels of the stress inducible HSP70 (upper panel) are comparable in wild type and *hrp36* null. Western blot of total larval protein challenged with the 7Fb antibody to detect stress-inducible Hsp70 in control (C), heat shocked larvae (HS) and in those that recovered from heat shock for 2 h (R). The lower panel shows the levels of β-tubulin in the corresponding samples.

3.9 *Levels of hsrω-n transcripts are enhanced by heat shock equally in wild type and hrp36 null larval SG but the splicing of the hsrω-n1 transcripts is affected in absence of Hrp36*

Semi-quantitative RT-PCR to assess the levels of hsrω-n in control and heat-shocked wild type and *hrp36* null larval SG showed almost equal enhancement following heat shock in both genotypes (figure 11). Interestingly, however, while in wild type heat-shocked glands, the spliced hsrω-n2 transcripts were more abundant than the unspliced hsrω-n1 species, in heat-shocked *hrp36* null SG, the unspliced form was more abundant than the spliced hsrω-n2 form, suggesting that in the absence of Hrp36, splicing of hsrω-n1 transcripts is compromised in heat shocked SG cells (figure 11).

4. Discussion

The *Df(3R)Hrb87F* is a small deletion that removes most of the Hrp36-encoding gene and an adjacent gene, *Tsr,* which is essential for male fertility (Zu *et al.* 1996; Haynes *et al.* 1997). Haynes *et al.* (1997) reported that *Df(3R)Hrb87F* homozygous flies are viable, and females fertile but males sterile. The sterility of *Df(3R)Hrb87F* homozygous males is rescued by a *P[Tsr]* transgene inserted on chromosome 2 (Haynes *et al.* 1997) so that *P[Tsr]/P[Tsr]; Df(3R)Hrb87F/Df(3R)Hrb87F* (*hrp36* null) stock can be maintained. Survival of organisms without the abundantly and universally expressed Hrp36 protein was suggested to be due to the functional redundancy with Hrp38, which shows 76%

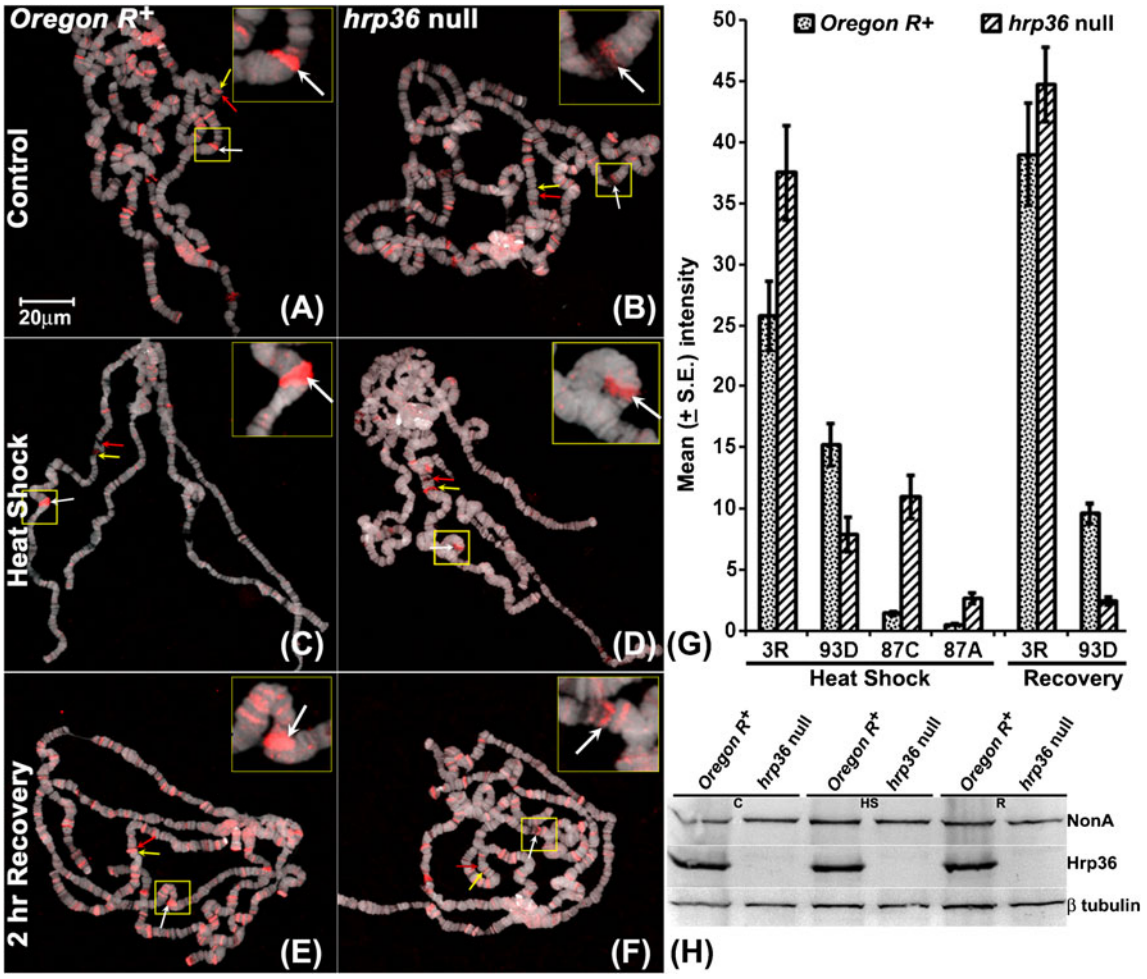

Figure 9. Immunolocalization of NonA protein (red) on salivary gland polytene chromosomes (white) in wild type and *hrp36* null (mentioned above each column) during control (**A** and **B**), 40 min heat shock at 37°C (**C** and **D**) and 2 h recovery from 40 min heat shock at 37°C (**E** and **F**) conditions. The white arrow indicates 93D locus, while red and yellow arrows indicate the 87A and 87C loci, respectively. (**G**) Graphical presentation of the amount of NonA on polytene chromosome 3R segment (100F to 93E), 93D, 87A and 87C puffs immediately after heat shock and on the 3R segment and the 93D puff after 2 h recovery from heat shock in wild type and *hrp36* null chromosome spreads (N=12 for each genotype). (**H**) Western blot showing the levels of NonA (top row) and Hrp36 (middle row) proteins in wild type and *hrp36* null salivary glands in control (C), after heat shock (HS), and after 2 h recovery from heat shock (R). Levels of β tubulin, used as loading control, are seen in the lower row. As expected, Hrp36 is completely absent in *hrp36* null in all given condition.

identity to RNP (RRM1) domain and 67% identity to the glycine-rich domain (GRD) of Hrp36 (Haynes *et al*. 1990, 1991; Zu *et al*. 1996). Although the initial studies by Haynes *et al*. (1997) indicated that the *hrp36* null individuals are without any apparent phenotype and viable, an earlier study in our laboratory (Sengupta and Lakhotia 2006) reported that eyes of *hrp36* null individuals show roughening due to loss of photoreceptors and that the *Df(3R)Hrb87F* acts as a dominant enhancer of neurodegeneration caused by expanded polyQ proteins in fly models. Our present study reveals that *hrp36* null individuals suffer from several other sub-lethal phenotypic consequences like developmental delay, altered site selection for pupation, significantly compromised female fecundity, reduced starvation and thermo-tolerance, etc. None of these phenotypes are due to the absence of the endogenous *Tsr* gene or to the presence of the *P[Tsr]* transgene insertion on chromosome 2 since we found that individuals homozygous for *Df(3R)Hrb87F* but not carrying the *P[Tsr]* transgene on chromosome 2 also displayed comparable defects (data not presented), although such males were, as expected, sterile (Haynes *et al.* 1997). It may be mentioned here that Manita *et al*. (2011) did not report any delay in development of $Hrb87F^{KG02089}$ and $Hrb87F^{BG02743}$ mutants because they compared the number of wild type and the *Hrb87F* mutant flies that had eclosed by day 15 without considering earlier time points. When grown at

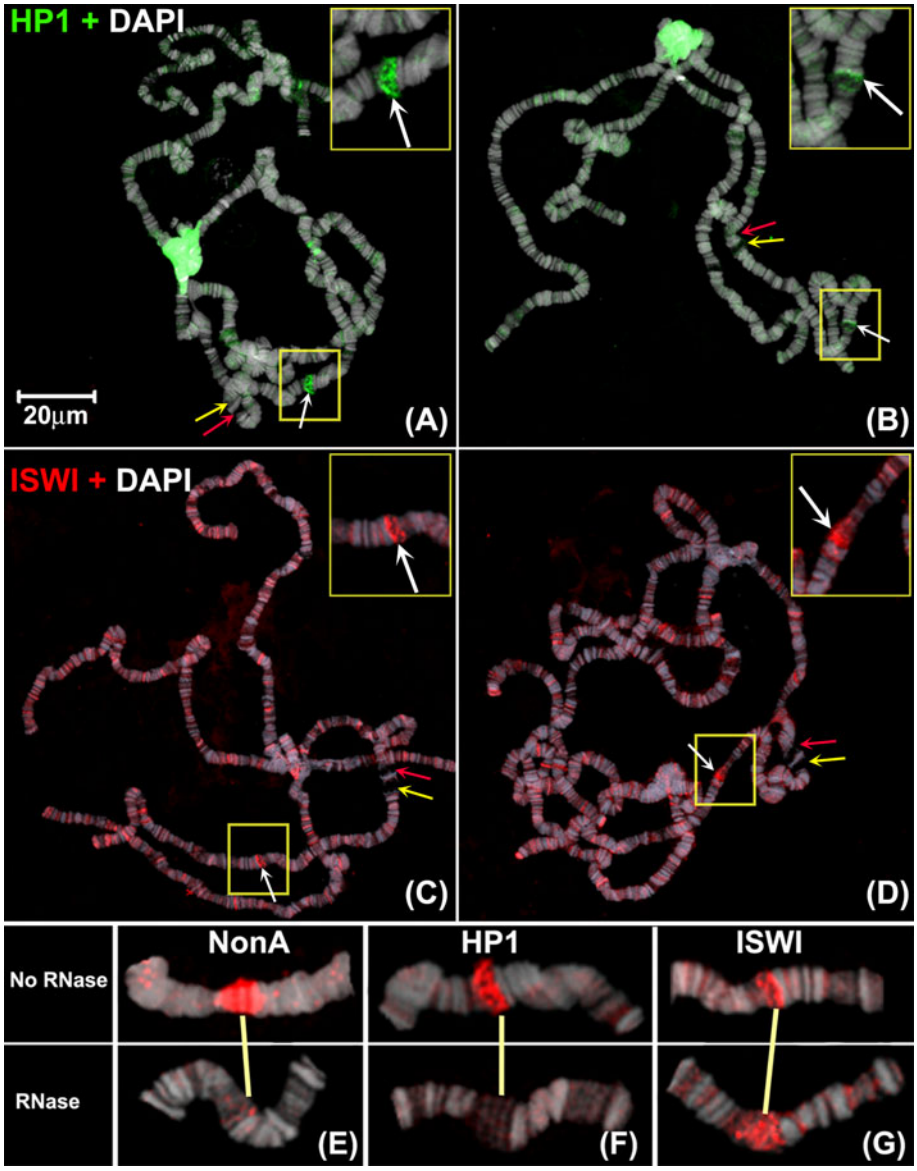

Figure 10. Confocal images showing the localization of HP1 (green) and ISWI (red) on salivary gland polytene chromosome (white) after 40 min of heat shock in wild type (**A** and **C**) and *hrp36* null (**B** and **D**). Higher magnification images are shown in insets. White, yellow and red arrows indicate 93D, 87C and 87A sites, respectively. Immunolocalization of NonA (**E**), HP1 (**F**) and ISWI (**G**) after heat shock (upper panel) and heat shock followed by RNase treatment (lower panel) at the 93D locus in wild type: levels of NonA and HP1 were dramatically reduced while those of ISWI remained unchanged after the *in vivo* RNAse treatment.

24°C, all *hrp36* null pupae emerge by day 15, while all the *Oregon* R^+ flies emerge by day 12 after embryo hatching. Therefore, Manita *et al*. (2011) would have missed the developmental delay seen in *hrp36* nulls. Thus, we suggest that notwithstanding the high degree of homology between Hrp36 and Hrp38 (Haynes *et al*. 1991, 1997), Hrp36 is not fully dispensable but is essential for normal development and female fecundity and, more importantly, for surviving stresses.

The nucleoplasmic omega speckles, organized by the nucleus limited long noncoding hsrω-n transcripts, help regulate the functional availability of a variety of hnRNPs and some other RNA-processing proteins (Lakhotia *et al*. 1999; Prasanth *et al*. 2000; Jolly and Lakhotia 2006; Mallik and Lakhotia 2011; Lakhotia 2011). Since we found the speckled pattern of nucleoplasmic hsrω-n RNA and the omega-speckle-associated proteins like NonA and Bancal to be nearly completely disrupted, it appears that, like the hsrω-n

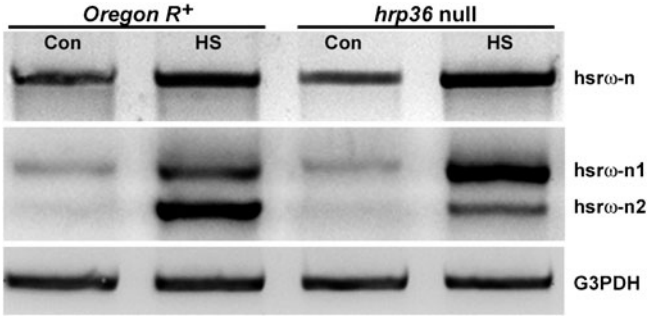

Figure 11. Absence of Hrp36 affects splicing of hsrω-n transcripts. RT-PCR amplicons showing the levels of total hsrω-n and its unspliced hsrω-n1 and spliced hsrω-n2 transcripts in control (Con) and after heat shock (HS) in wild type and *hrp36* null salivary glands. G3PDH amplicons (lowest row) of corresponding samples were used as loading control to normalize the amount of hsrω-n transcripts.

transcripts (Prasanth *et al*. 2000; Mallik and Lakhotia 2011), Hrp36 is also a core constituent of omega speckles. A physical interaction of Hrp36 with hsrω transcripts in omega speckles was shown through the presence of these transcripts in Hrp36-immunoprecipitate (Prasanth *et al*. 2000; Mallik and Lakhotia 2011). The RBD-2 and GRD of Hrp36 are reported to show high affinity binding with UAGGUUAGG, which is very similar to the conserved nonamer AUAG-GUAGG present at ~100 b intervals in the repeats present in the hsrω-n transcripts (Mayeda *et al*. 1998; Zu *et al*. 1998). Thus, it appears that Hrp36 directly binds with the hsrω-n transcripts and the two together provide the core platform for other proteins to assemble at omega speckles. However, proteins like NonA can still associate with the hsrω transcripts since the heat-shock-induced accumulation at the 93D puff in *hrp36* null cells, although less than in cells that have Hrp36, was found to be sensitive to RNAse.

The observed effect on the distribution and abundance of the nuclear-matrix-associated protein like Megator may be a consequence of the well-known association of hnRNP A with the nuclear matrix (He *et al*. 1991; Zimowska *et al.* 1997). The enhanced levels of Megator in nuclear matrix in the endoreplicated MT nuclei does not appear to be simply due to the increased DNA content in *hrp36* null MT cells since the ratio of fluorescence intensities of nucleoplasmic Megator and DNA (DAPI) in the *hrp36* null principal cells was several folds greater than in corresponding wild type MT. The disruption of omega speckles in *hrp36* null cells may also be related to the altered organization of nuclear matrix since these speckles are associated with the nuclear matrix (our unpublished observations). Additionally, the observed increase in the ISWI content in *hrp36* nulls may also affect omega speckles since this chromatin remodeller is known to be involved in organizing omega speckles (Onorati *et al*. 2011). These possibilities need further studies.

In the absence of organized omega speckles, the regulated availability of a variety of hnRNPs and other RNA-processing proteins for different cellular events in all body cells is expected to be compromised (Mallik and Lakhotia 2011; Lakhotia *et al*. 2012). Such a global effect of the absence of organized omega speckles on the orderly availability of nuclear RNA-processing proteins and the above-noted involvement of Hrp36 in processing of a large number of nuclear RNA species is expected to affect timely progression of several cellular processes, which cumulatively result in varyingly delayed development of *hrp36* null organisms. Ji and Tulin (2012) recently reported that depletion of Hrp38 causes substantial pre-pupal lethality. On the other hand, we found that a complete absence of Hrp36 slows down the development but does not affect larval or pupal survival, although the adult life span is reduced. Therefore, it appears that because of the buffering of Hrp36 functions by the other hnRNP A1 homologs, its complete absence does not cause larval or pupal death under normal developmental conditions but still has a sub-lethal effect.

The Hrp36, together with hsrω-n RNA and omega-speckle-associated proteins like the Hrp40/Squid, Hrp48/Hrb27C, etc., is abundantly expressed during oogenesis (Mutsuddi and Lakhotia 1995; Lakhotia *et al*. 2001; Norvell *et al*. 2005). Although a number of hnRNPs have been shown to perform specific functions during oogenesis in *Drosophila*, including localization and translation of antero-posterior axis determining transcripts and proteins (Goodrich *et al*. 2004; Steinhauer and Kalderon 2005; Norvell *et al*. 2005; Geng and MacDonald 2006; Clouse *et al*. 2008; Ji and Tulin 2012), a specific role of Hrp36 in ovary development and oogenesis is not yet known. Our results show that in the absence of Hrp36, the overall development of ovaries is affected so that fewer ovarioles are formed and among them also, many of the follicles fail to complete differentiation resulting in the overall reduced fecundity. Involvement of Hrp36 in early differentiation of ovary is also indicated by the unequal size of two ovaries in *hrp*36 null females. It appears that the other related hnRNPs like Hrp38, Hrp40 and Hrp48 cannot completely compensate for the complete absence of Hrp36 so that under the limiting conditions, only one of the developing ovaries is able to attain a threshold state for differentiation of ovarioles to some extent. A global overexpression of hsrω transcripts because of the *Act5C-GAL4*-driven expression of the *EP3037* allele of *hsrω*, which sequesters a greater amount of hnRNPs in omega speckle clusters resulting in their functional depletion (Mallik and Lakhotia 2009, 2011), also results in unequal size of the two ovaries with greatly reduced numbers of follicles and mature eggs (Soundarya Iyer, Moushami Mallik and SC Lakhotia, unpublished). Significantly, depletion of Hrp38 is not reported to result in development of unequal sized ovaries although the stem cell maintenance and oocyte location are affected (Ji and Tulin 2012). Hrp36, therefore, appears to be involved in other

events of early steps of development and differentiation of ovarioles. The observed alterations in the F-actin in the *hrp36* null ovarioles may also contribute to mis-organized egg chambers. The failure of chromatin dispersal in *hrp36* null nurse cells older than stage 5 (King 1970; Dej and Spradling 1999) is comparable to that seen in *Hrb27C*, *Squid* or *otu* mutants (King *et al*. 1981; King and Storto 1988; Goodrich *et al*. 2004). Therefore, it appears that these proteins may act in concert to bring about the dispersal of nurse cell chromatin before the stage 6. All these factors together contribute to poor growth and consequent apoptosis of egg chambers at stage 7–8. Although the *hrp36* null egg chambers that progress beyond stage 7–8, and develop to apparently normal-looking eggs, the observed maternal effect leading to embryonic death of ~17–18% of eggs laid by *hrp36* null mothers clearly indicates a continuing role of Hrp36 protein in later stages of oogenesis, which can only be partially compensated by the other hnRNPs. Further studies are required to understand the specific roles of Hrp36 in differentiation of ovaries and egg chambers.

It is unlikely that the additional endoreplication cycles in MT cells is a direct consequence of the longer period of development of the *hrp36* null larvae since several other mutations that prolong the larval period are not known to show enhanced levels of polyteny in MT cells. Since a unique feature of larval MT is that it continues as such in adults without histolysis during pupal metamorphosis, the regulation of endoreplication cycles in MT is different from that in the other endoreplicating larval tissues which histolyse following the pupal moult. Enhanced polyteny and consequent larger nuclear size in principal cells of MT nuclei and persistence of blob-like forms of endoreplicated advanced stage nurse cell nuclei suggest a possible role of Hrp36 in higher-order chromatin organization in at least some of the endoreplicating nuclei. In this context, it is significant that Manita *et al*. (2011) have shown a direct interaction between Hrp36 and DNA topoisomerase I. The cytologically analysable polytene chromosomes in MT of *hrp36* null individuals provide, besides the classically used salivary gland polytene chromosomes, an additional tissue for studies on gene expression at chromosomal level in *Drosophila*.

The substantial extension of telomeres of most chromosomes in *hrp36* null larval SG is remarkable. Hrp36 and other hnRNPs are known to be present at polytene telomeres (Lakhotia *et al*. 2012) and hnRNPs are known to be involved in telomere organization in mammalian cells (He and Smith 2009). Further studies on the role of Hrp36 in telomere maintenance in *Drosophila* are currently in progress and would be reported elsewhere.

It is significant that as observed earlier in the case of *hsrω*-deficient or *hsrω*-overexpressing individuals (Lakhotia *et al*. 2012), the *hrp36* null larvae and adults also display high sensitivity to elevated temperature in spite of the characteristic inducion of the heat shock puffs and the induced synthesis of Hsp70. Besides the induction of heat shock genes, the well-documented dynamic relocalization of omega speckles and their associated hnRNPs following heat shock and during subsequent recovery from the stress (Lakhotia *et al*. 1999; Prasanth *et al*. 2000) is equally essential for surviving the thermal stress (Lakhotia *et al*. 2012). Although the relocalization of omega-speckle-associated NonA or the HP1 protein on general chromosome regions following recovery from heat shock was not as severely affected in the *hrp36* null cells as when the omega speckles were disrupted because of down-regulation or absence of the hsrω-n transcripts (Lakhotia *et al*. 2012), the association of these proteins at the *hsrω* gene locus and the reformation of omega speckles were affected in *hrp36* null cells. Therefore, Hrp36, like the hsrω-n transcripts (Lakhotia *et al*. 2012), has an essential role in the dynamic redistribution of proteins like NonA and HP1 following stress and recovery from stress, and therefore, its absence results in high sensitivity to stress.

Although ISWI, an important member of chromatin remodelling complexes, is required for assembly of typical omega speckles (Onorati *et al*. 2011), its accumulation at the *hsrω* gene site (93D puff) following heat shock was not found to be affected by the absence of Hrp36. Since RNAse treatment of live SG did not affect its presence at the 93D site, ISWI seems to be associated with chromatin rather than with the heat-shock-induced hsrω transcripts with which HP1 and NonA proteins are bound. Sala *et al*. (2008) reported that ISWI, which normally binds with the uninduced *hsp70* DNA at 87A and 87C sites, gets displaced as chromatin contents of these puffs get increasingly poly-ADP-ribosylated (PARylated) following heat shock. In contrast, the ISWI protein's level at the 93D site was more abundant at the 93D puff in heat-shocked cells (figure 10C, D and G). Interestingly, we noticed that ISWI is also present at heat shock puffs other than the 87A and 87C (details not shown, but see figure 10C and D). This difference in the association of ISWI with heat-shock-induced 87A/87C puffs on one hand and the 93D and other heat shock puffs on the other, requires further study.

Ji and Tulin (2009) suggested that heat-shock-induced PARylation of chromatin associated hnRNPs causes these hnRNPs to come to nucleoplasm where they get de-PARylated and thus finally get sequestered at the 93D puff site because the de-PARylated hnRNPs associate with hsrω-n transcripts. In this context, it remains to be examined if the reduced levels of proteins like NonA at the 93D puff after heat shock in the *hrp36* null cells is due to inefficient de-PARylation of these proteins in the absence of Hrp36 or due to a direct role of Hrp36 in the movement of other hnRNPs and NonA, etc., to the 93D puff after heat shock.

In agreement with the report of Ji and Tulin (2009) that in poly(ADP-ribose) glycohydrolase (PARG)-deficient cells,

which accumulate much less hnRNPs at the 93D puff after heat shock, the splicing of *hsrω* nuclear transcripts to remove the intron is affected in *hrp36* null cells as well. It may be noted here that while the RT-PCR primers used in Ji and Tulin's (2009) study could not discriminate between splicing of the hsrω-n (hsrω-RB) and hsrω-pre-c (hsrω-RA) transcripts, the primers designed by Mallik and Lakhotia (2011) and used in the present study unambiguously identify that splicing of hsrω-n (hsrω-RB) transcript is affected in the *hrp36* null cells. The effect on splicing on the hsrω-n transcripts in *hrp36* null cells agrees with the known role of Hrp36 in alternative splicing (Zu *et al*. 1996, 1998; Olson *et al*. 2007; Borah *et al*. 2009; Blanchette *et al*. 2009; Nilsen and Graveley 2010). The functional consequences of retention of intron in the hsrω-n1 transcript on recovery from heat shock remain to be analysed.

A role of Hrp36 in starvation tolerance is indicated by our studies, although the underlying mechanism is not clear. It is to be expected that starvation stress would affect cell physiology, gene expression and RNA processing in many ways, some or all of which may involve the hnRNPs. For example Griffith *et al.* (2006) have shown a role of hnRNP A and some other hnRNPs in regulating splicing of G6PD during starvation in mice. In another study in our lab (Dwivedi *et al.* 2012), an association has been found between enhanced levels of hnRNPs (including Hrp36), faster development and improved tolerance against starvation and thermal stresses. Present results are in agreement with these findings since absence of Hrp36 is associated with delayed development and poor stress tolerance.

In view of the very wide variety of functions mediated by hnRNP A1 family members in eukaryotic cells (Martinez-Contreras *et al*. 2007; He and Smith 2009; Chaudhury *et al*. 2010; Han *et al*. 2010; Nilsen and Graveley 2010), it is not surprising that a complete absence of the Hrp36 has such pleiotropic, although sub-lethal, phenotypic consequences. Interestingly, while its complete absence does not have lethal consequences under normal laboratory developmental conditions presumably because of the overlapping functions provided by related hnRNPs like Hrp38, Hrp40 and Hrp48, the *hrp36* null condition is highly detrimental under unfavourable conditions like starvation and thermal stresses. We believe that this essential requirement of Hrp36 under conditions of stress is primarily because of its interaction with the hsrω-n transcripts to organize the omega speckles and facilitate the recruitment of other proteins to omega speckles. Since environmental stresses exert strong selection force under natural conditions, and since the roles of Hrp36 under stress cannot be complemented by the other related hnRNPs, the *hrp36* gene is retained in the fly genome. Persistence of multiple members of a given family of hnRNP in higher eukaryotes indicates that while they share common structural and functional properties, each one also performs certain unique sets of functions that are essential for the fine tuning of cell's activities in relation to requirements of differentiation and environmental conditions.

Acknowledgements

We thank Dr Susan Hayness for the *Df(3R)Hrb87F* fly stock and Dr H Saumweber (Berlin, Germany) for P11, Q18, Bj6, Bx34 antibodies, Dr M B Evgen'ev (Russia) for 7Fb antibody and D Corona (Italy) for ISWI antibody. The work was supported by the Department of Science & Technology, New Delhi, through the Ramanna Fellowship and the National Facility for Confocal Microscopy grants to SCL. AKS is supported through Research Fellowship from the CSIR.

Note added in proof Subsequent to acceptance of this paper, we have examined the effect of expression of FLAG-tagged full length Hrp36 under a leaky Hsp70 promoter (Zu *et al*. 1996) in otherwise *hrp36* null background. The leaky expression of one copy of the FLAG-tagged full length Hrp36 in otherwise *hrp36* null embryos, grown at 24°C or at 30°C, almost fully complements all the phenotypes noted in this study for the *hrp36* nulls, except the elongated telomeres. These results confirm that the different phenotypes described here for the *hrp36* null individuals are indeed due to absence of the Hrp36 protein.

References

Blanchette M, Green RE, MacArthuer S, Brooks AN, Brenner SE, Eisen MB and Rio DC 2009 Genome-wide analysis of alternative Pre-mRNA splicing and RNA-Binding specificities of the Drosophila hnRNP A/B family members. *Mol. Cell* **33** 438–449

Boehm AK, Saunders A, Werner J and Lis JT 2003 Transcription factor and polymerase recruitment, modification, and movement on dhsp70 in vivo in the minutes following heat shock. *Mol. Cell Biol*. **23** 7628–7637

Bonner JJ and Kerby RL 1982 RNA polymerase II transcribes all of the heat shock induced genes of *Drosophila melanogaster*. *Chromosoma* **85** 93–108

Borah S, Wong AC and Steitz JA 2009 *Drosophila* hnRNP A1 homologs Hrp36/Hrp38 enhance U2-type versus U12-type splicing to regulate alternative splicing of the prospero twintron. *Proc. Natl. Acad. Sci. USA* **106** 2577–2582

Busch A and Hertel KJ 2012 Evolution of SR protein and hnRNP splicing regulatory factors. *WIREs RNA* **3** 1–12

Chaudhury A, Chander P and Howe PH 2010 Heterogeneous nuclear ribonucleoproteins (hnRNPs) in cellular processes: Focus on hnRNP E1's multifunctional regulatory roles. *RNA* **16** 1449–1462

Clouse KN, Ferguson SB and Schupbach T 2008 Squid, Cup, and PABP55B function together to regulate gurken translation in *Drosophila*. *Dev. Biol.* **313** 713–724

Corona DFV, Siriaco G, Armstrong JA, Snarskaya N, McClymont SA, Scott MP and Tamkun JW 2007 ISWI regulates higher-

order chromatin structure and histone H1 assembly in vivo. *PLoS Biol.* **5** e232

Daneholt B 2001 Assembly and transport of a premessenger RNP particle. *Proc. Natl. Acad. Sci. USA* **98** 7012–7017

Dej KJ and Spradling AC 1999 The endocycle controls nurse cell polytene chromosome structure during *Drosophila* oogenesis. *Development* **126** 293–303

Dwivedi V, Anandan EM, Mony RS, Muraleedharan TS, Valiathan MS, Mutsuddi M and Lakhotia SC 2012 *In vivo* effects of traditional Ayurvedic formulations in *Drosophila melanogaster* model relate with therapeutic applications. *PLos One* **7** e37113

Geng C and Macdonald PM 2006 Imp associates with squid and Hrp48 and contributes to localized expression of gurken in the oocyte. *Mol. Cell Biol.* **26** 9508–9516

Gerber M, Tenney K, Conaway JW, Conaway RC, Eissenberg JC and Shilatifard A 2005 Regulation of heat shock gene expression by RNA polymerase II elongation factor, Elongin A. *J. Biol. Chem.* **280** 4017–4020

Goodrich JS, Clouse KN and Schupbach T 2004 Hrb27C, Sqd and Otu cooperatively regulate gurken RNA localization and mediate nurse cell chromosome dispersion in *Drosophila* oogenesis. *Development* **131** 1949–1958

Griffith BN, Walsh CM, Szeszel-Fedorowicz W, Timperman AT and Salati LM 2006 Identification of hnRNPs K, L and A2/B1 as candidate proteins involved in the nutritional regulation of mRNA splicing. *Biochim. Biophys. Acta.* **1759** 552–561

Guisbert KK, Duncan K, Li H and Guthrie C 2005 Functional specificity of shuttling hnRNPs revealed by genome-wide analysis of their RNA binding profiles. *RNA* **11** 383–393

Han SP, Kassahn KS, Skarshewski A, Ragan MA, Rothnagel JA and Smith R 2010 Functional implications of the emergence of alternative splicing in hnRNP A/B transcripts. *RNA* **16** 1760–1768

Haynes SR, Cooper MT, Pype S and Stolow DT 1997 Involvement of a tissue-specific RNA recognition motif protein in *Drosophila* spermatogenesis. *Mol. Cell Biol.* **17** 2708–2715

Haynes SR, Johnson D, Raychaudhuri G and Beyer AL 1991 The *Drosophila Hrb87F* gene encodes a new member of the A and B hnRNP protein group. *Nucleic Acids Res*. **19** 25–31

Haynes SR, Raychaudhuri G and Beyer AL 1990 The *Drosophila Hrb98DE* locus encodes four protein isoforms homologous to the A1 protein of mammalian heterogeneous nuclear ribonucleoprotein complexes. *Mol. Cell Biol.* **10** 316–323

He DC, Martin T and Penman S 1991 Localization of heterogeneous nuclear ribonucleoprotein in the interphase nuclear matrix core filaments and on perichromosomal filaments at mitosis. *Proc. Natl. Acad. Sci. USA* **88** 7469–7473

He Y and Smith R 2009 Nuclear functions of heterogeneous nuclear ribonucleoproteins A/B *Cell. Mol. Life Sci.* **66** 1239–1256

Ji Y and Tulin AV 2009 Poly(ADP-ribosyl)ation of heterogeneous nuclear ribonucleoproteins modulates splicing. *Nucleic Acids Res.* **37** 3501–3513

Ji Y and Tulin AV 2012 Poly(ADP-ribose) controls DE-cadherin-dependent stem cell maintenance and oocyte localization. *Nat. Commun.* **3** 760 doi: 10.1038 ncomms1759

Jolly C and Lakhotia SC 2006 Human sat III and *Drosophila* hsr omega transcripts: a common paradigm for regulation of nuclear RNA processing in stressed cells. *Nucleic Acids Res.* **34** 5508–5514

King RC 1970 The meiotic behavior of the *Drosophila* oocyte. *Int. Rev. Cytol.* **28** 125–168

King RC, Riley SF, Cassidy JD, White PE and Paik YK 1981 Giant polytene chromosomes from the ovaries of a *Drosophila* mutant. *Science* **212** 441–443

King RC and Storto PD 1988 The role of the otu gene in *Drosophila* oogenesis. *Bioessays* **8** 18–24

Kozlova N, Braga J, Lundgren J, Rino J, Young P, Carmo-Fonseca M and Visa N 2006 Studies on the role of NonA in mRNA biogenesis. *Exp. Cell Res.* **312** 2619–2630

Lakhotia SC 1974 EM Autoradiographic Studies on polytene nuclei *of Drosophila melanogaster* III. Localisation of non-replicating chromatin in the chromocentre heterochromatin. *Chromosoma* **46** 145–159

Lakhotia SC 1984 Replication in *Drosophila* chromosomes XII. Reconfirmation of underreplication of heterochromatin in polytene nuclei by cytofluorometry. *Chromosoma* **89** 63–67

Lakhotia SC 2003 Integration of transcriptional and translational activities in normal and stressed cells by the noncoding hsr-omega transcripts in *Drosophila. Biol. Intl.* **45** 30–33

Lakhotia SC 2011 Forty years of the 93D puff of *Drosophila melanogaster*. *J. Biosci*. **36** 399–423

Lakhotia SC, Mallik M, Singh AK and Ray M 2012 The large noncoding hsromega-n transcripts are essential for thermotolerance and remobilization of hnRNPs, HP1 and RNA polymerase II during recovery from heat shock in *Drosophila*. *Chromosoma* **121** 49–70

Lakhotia SC, Rajendra TK and Prasanth KV 2001 Developmental regulation and complex organization of the promoter of the noncoding hsr(omega) gene of *Drosophila melanogaster*. *J. Biosci.* **26** 25–38

Lakhotia SC, Ray P, Rajendra TK and Prasanth KV 1999 The noncoding transcripts of *hsr-omega* gene in *Drosophila*: Do they regulate trafficking and availability of nuclear RNA-processing factors? *Curr. Sci.* **77** 553–563

Lakhotia SC and Tapadia MG 1998 Genetic mapping of the amide response element(s) of the hsr omega locus of *Drosophila melanogaster*. *Chromosoma* **107** 127–135

Mallik M and Lakhotia SC 2009 The developmentally active and stress-inducible noncoding hsromega gene is a novel regulator of apoptosis in *Drosophila*. *Genetics* **183** 831–852

Mallik M and Lakhotia SC 2010 Improved activities of CREB binding protein, heterogeneous nuclear ribonucleoproteins and proteasome following downregulation of noncoding hsromega transcripts help suppress poly(Q) pathogenesis in fly models. *Genetics* **184** 927–945

Mallik M and Lakhotia SC 2011 Pleiotropic consequences of misexpression of the developmentally active and stress-inducible non-coding hsromega gene in *Drosophila*. *J. Biosci.* **36** 265–280

Manita D, Toba Y, Takakusagi Y, Matsumoto Y, Kusayanagi T, Takakusagi K, Tsukuda S, Takada K, Kanai Y, Kamisuki S, Sakaguchi K and Sugawara F 2011 Camptothecin (CPT) directly binds to human heterogeneous nuclear ribonucleoprotein A1 (hnRNP A1) and inhibits the hnRNP A1/topoisomerase I interaction. *Bioorg. Med. Chem.* **19** 7690–7697

Martinez-Contreras R, Cloutier P, Shkreta L, Fisette JF, Revil T and Chabot B 2007 hnRNP proteins and splicing control. *Adv. Exp. Med. Biol.* **623** 123–147

Mayeda A, Munroe SH, Xu RM and Krainer AR 1998 Distinct functions of the closely related tandem RNA-recognition motifs of hnRNP A1. *RNA* **4** 1111–1123

Mutsuddi M and Lakhotia SC 1995 Spatial expression of the hsr-omega (93D) gene in different tissues of *Drosophila melanogaster* and identification of promoter elements controlling its developmental expression. *Dev. Genet.* **17** 303–311

Nilsen TW and Graveley BR 2010 Expansion of the eukaryotic proteome by alternative splicing. *Nature* **463** 457–463

Norvell A, Debec A, Finch D, Gibson L and Thoma B 2005 Squid is required for efficient posterior localization of oskar mRNA during Drosophila oogenesis. *Dev. Genes Evol.* **215** 340–349

Olson S, Blanchette M, Park J, Savva Y, Yeo GW, Yeakley JM, Rio DC and Graveley BR 2007 A regulator of Dscam mutually exclusive splicing fidelity. *Nat. Struct. Mol. Biol.* **14** 1134–1140

Onorati MC, Lazzaro S, Mallik M, Ingrassia AM, Carreca AP, Singh AK, Chaturvedi DP, Lakhotia SC and Corona DFV 2011 The ISWI chromatin remodeler organizes the hsromega ncRNA-containing omega speckle nuclear compartments. *PLoS Genet.* **7** e1002096

Piacentini L, Fanti L, Negri R, Del Vescovo V, Fatica A, Altieri F and Pimpinelli S 2009 Heterochromatin protein 1 (HP1a) positively regulates euchromatic gene expression through RNA transcript association and interaction with hnRNPs in *Drosophila*. *PLoS Genet.* **5** e1000670

Prasanth KV, Rajendra TK, Lal AK and Lakhotia SC 2000 Omega speckles - a novel class of nuclear speckles containing hnRNPs associated with noncoding hsr-omega RNA in *Drosophila*. *J. Cell Sci.* **113** 3485–3497

Sala A, La Rocca G, Burgio G, Kotova E, Di Gesu D, Collesano M, Ingrassia AM, Tulin AV and Corona DFV 2008 The nucleosome-remodeling ATPase ISWI is regulated by poly-ADP-ribosylation. *PLoS Biol.* **6** e252

Saumweber H, Symmons P, Kabisch R, Will H and Bonhoeffer F 1980 Monoclonal antibodies against chromosomal proteins of *Drosophila melanogaster*: establishment of antibody producing cell lines and partial characterization of corresponding antigens. *Chromosoma* **80** 253–275

Sengupta S and Lakhotia SC 2006 Altered expressions of the noncoding hsromega gene enhances poly-Q-induced neurotoxicity in *Drosophila*. *RNA Biol.* **3** 28–35

Sofola OA, Jin P, Qin Y, Duan R, Liu H, de Haro M, Nelson DL and Botas J 2007 RNA-binding proteins hnRNP A2/B1 and CUGBP1 suppress fragile X CGG premutation repeat-induced neurodegeneration in a *Drosophila* model of FXTAS. *Neuron* **55** 565–571

Steinhauer J and Kalderon D 2005 The RNA-binding protein Squid is required for the establishment of anteroposterior polarity in the *Drosophila* oocyte. *Development* **132** 5515–5525

Velazquez JM and Lindquist S 1984 hsp70: nuclear concentration during environmental stress and cytoplasmic storage during recovery. *Cell* **36** 655–662

Zeng C, Kim E, Warren SL and Berget SM 1997 Dynamic relocation of transcription and splicing factors dependent upon transcriptional activity. *EMBO J.* **16** 1401–1412

Zimowska G, Aris JP and Paddy MR 1997 A *Drosophila* Tpr protein homolog is localized both in the extrachromosomal channel network and to nuclear pore complexes. *J. Cell Sci.* **110** 927–944

Zimowska G and Paddy MR 2002 Structures and dynamics of *Drosophila* Tpr inconsistent with a static, filamentous structure. *Exp. Cell Res.* **276** 223–232

Zu K, Sikes ML and Beyer AL 1998 Separable roles in vivo for the two RNA binding domains of a *Drosophila* A1-hnRNP homolog. *RNA* **4** 1585–1598

Zu K, Sikes ML, Haynes SR and Beyer AL 1996 Altered levels of the *Drosophila* HRB87F/hrp36 hnRNP protein have limited effects on alternative splicing in vivo. *Mol. Biol. Cell* **7** 1059–1073

MS received 20 April 2012; accepted 19 June 2012

Corresponding editor: PRIM B SINGH